Soft X-ray FEL Seeding Studies for LCLS-II: Task Force Status Report

A White Paper by SLAC and LBNL

E. Hemsing[1], R. Coffee[1], G. Dakovski[1], W. M. Fawley[1], Y. Feng[1], B. Garcia[1], J. Hastings[1], Z. Huang[1], G. Marcus[1], G. Penn[2], D. Ratner[1], T. Raubenheimer[1], and R. W. Schoenlein[1]

[1]SLAC National Accelerator Laboratory
[2]Lawrence Berkeley National Laboratory

This material is based upon work supported by the U.S. Department of Energy, Office of Science, under Contract No. DE-AC02-76SF00515.

Table of Contents

Executive Summary

We present the current status of studies on the most promising options for soft x-ray seeding at LCLS-II. These are Echo Enabled Harmonic Generation (EEHG) and soft x-ray self seeding (SXRSS). Cascaded High Gain Harmonic Generation (HGHG) has also been examined in detail, but does not deliver on the expectations of spectral brightness, spectral purity, bandwidth, and tunability in the demanding 1-2 nm range. Several other seeding schemes have also been evaluated (e.g., direct seeding via High Harmonic Generation (HHG) and coherent Inverse Compton Scattering (ICS)), but at this stage are not considered promising, or are in need of extensive development to deliver on the identified performance goals.

The choice of seeding schemes is motivated by key photon science targets for 10-100 fs, Fourier transform-limited pulses with tunable time-bandwidth tradeoff in the soft x-ray regime. These are matched with overlapping performance expectations for the various seeding schemes based on theoretical studies, high-fidelity numerical simulations of start-to-end 100 & 300 pC beams for LCLS-II, ideal beams, and finally experimental experience with SXRSS at LCLS. Judged by these and other requirements which include resolving power, photon density, multicolor seeding, and spectral purity, early indications show EEHG and SXRSS are the leading candidates, though there are clear challenges with both schemes. These seeding options appear to be complementary and non-interfering, given the available space in the current LCLS-II beam line design, as well as expectations of user demand and FEL performance. Our preliminary assessment takes into account the existing SXRSS system and performance at LCLS and several already accomplished proof-of-principle EEHG studies. Further reduction of risk will hinge on necessary upcoming R&D, specifically experimental EEHG studies both at FERMI (Trieste, Italy) and at SXFEL (Shanghai, China), additional numerical simulation studies with seeding-optimized LCLS-II beams, further analytic studies, and the technical development of a high-rep rate LCLS-II SXRSS system. As such, the anticipated advantages and disadvantages of each scheme are described, particularly as they pertain to the science drivers. A preliminary roadmap for critical R&D is also presented.

Overview

In this White Paper we report on the present status of LCLS-II FEL external laser seeding studies that have been conducted as part of a dedicated joint SLAC/LBNL FEL Seeding Task Force starting in FY 2016. The goal of the Task Force is to evaluate the status and prospects of numerous soft x-ray seeding options for LCLS-II and compare their projected performance against the requirements as defined by the science drivers of greatest potential impact. This White Paper summarizes the progress at this halfway point of the Task Force's nominal lifetime in surveying the evolving capabilities and potentials of different schemes, and in particular how they could enable critical new science opportunities beyond the LCLS-II baseline design. We identify the highest-impact photon science techniques that require Fourier transform-limited pulses at 1-4 nm output wavelength, and compare their requirements with the expected performance of the leading seeding schemes, including external laser seeding and self-seeding. We then describe the next level R&D required to downselect a seeding scheme and lay out a detailed design for LCLS-II. This effort aims to keep current and future US FEL facilities at the forefront of X-ray science as is central to the BES mission. Specifically, it:

- Identifies the critical scientific aspects of seeding implementation that have the greatest potential to enhance the impact of the LCLS-II X-ray FEL facility
- Presents a summary of recent seeding studies and compares the performance of different schemes based on high-fidelity simulations of both ideal and start-to-end beams for LCLS-II
- Identifies the overall performance goals for seeding, the anticipated potential for each scheme, the

current challenges and issues, and near-term studies

- Describes upcoming collaborative experimental studies at international institutions (FERMI, SXFEL, and sFLASH) that can directly inform external seeding at LCLS-II.

Motivation for Seeding

To date, most short wavelength FEL facilities have depended upon the well-known Self-Amplified Spontaneous Emission (SASE) mechanism to generate intense output pulses. Although SASE is relatively easy to implement, it has the drawback of providing output pulses whose fluence, spectrum, and coherence properties can vary strongly from shot-to-shot. In contrast, seeding (either via FEL self-seeding or via a well-controlled, external laser) offers the promise of nearly Fourier-transform limited and highly repeatable pulses in all major properties such as fluence, spectrum and central wavelength, and longitudinal coherence. External laser seeding (ELS) also includes the possibility of producing pulses with specified eikonal phase properties such as a wavelength chirp. Moreover, ELS can be used to define both the temporal duration of the output pulse essentially independent of the shot-to-shot variation of the electron beam pulse and the temporal centroid, this latter capability being useful for pump-probe experiments. Presuming a wavelength-tunable seed and variable gap undulators (as specified in the baseline proposal for LCLS-II), the FEL output pulse can be smoothly tuned in wavelength over time without requiring a change in the electron beam energy, as is presently required for LCLS. Finally, ELS allows the straightforward production of coherent multicolor, temporally-separate pulses in the soft x-ray range. Nearly all of these desirable properties have already been demonstrated experimentally at XUV wavelengths by the FERMI FEL-1 of Sincrotrone Trieste, albeit at much lower repetition rates (10 - 50 Hz) than is foreseen for LCLS-II.

Goal of the Task Force

The FEL Seeding Task Force was initiated to systematically compare all possible seeding schemes and ensure that LCLS-II does not preclude the most promising option. The task is to evaluate their scientific impact, status, and prospects for implementation in the 1-2 nm x-ray regime. Specifically, the mission is to survey the status of each seeding scheme, define beam and laser requirements, carry out high-fidelity simulations, plan and execute experiments to validate simulations, and to explore the limits of each method. The final goal is to down select an external seeding scheme, and lay out a detailed design for LCLS-II.

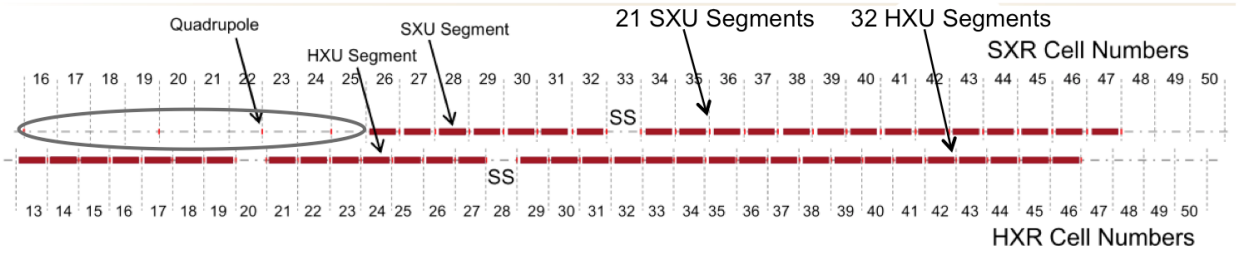

Figure 1: Layout of the LCLS-II soft x-ray (top) and hard x-ray (bottom) undulators. There is ~40 m of space available upstream of the soft x-ray line (circled) that could be used for external seeding infrastructure.

Parameter	Symbol	Value	Unit
Energy	E	4.0	GeV
Charge	Q	100-300	pC
Peak current	I	1.0	kA
Emittance	ϵ_n	4.5 x 10^{-7}	m-rad
Energy spread	σ_E	500	keV
Beta function	<β>	12 (13)	m

Parameter	Value SXR (HXR)	Unit
Type	Hybrid PM, planar	-
Full gap height	Variable	-
Period	39 (26)	mm
Segment length	3.4	m
Break length	1.0	m
# segments	21 (32)	-
Total length	96 (140)	m

Figure 2: Parameters of the LCLS-II soft x-ray beam (left) and x-ray undulators (right).

Current Status Summary

For the 4 GeV beams at LCLS-II, the most promising seeding options are Echo Enabled Harmonic Generation (EEHG) and soft x-ray self seeding (SXRSS) based on detailed simulations and performance potential. There are, however, clear challenges with both schemes, and upcoming studies and experiments will continue to inform this Task Force's recommendation for LCLS-II one year hence.

Scientific Opportunities with Transform-Limited Soft X-rays

General Motivation

The general motivation for soft X-ray FEL (external) seeding arises from the need for control over the longitudinal coherence (i.e. spectral amplitude and phase) of X-ray pulses for a broad range of science applications. In the soft X-ray range, time-resolved X-ray spectroscopy and time-resolved resonant X-ray scattering are powerful probes of excited-state dynamics in material and molecular complexes. The scientific impact of these methods relies on optimizing both the time resolution and the bandwidth (spectral resolution) for specific science requirements. The ability to trade-off time-resolution and spectral resolution at close to the Fourier transform limit will open new dimensions in X-ray science.

The most compelling experimental approaches and associated x-ray requirements are listed in Figure 3. One can outline a range of interest that will arguably satisfy the vast majority of science applications as follows:

High time resolution: 10 fs_{FWHM} ⇔ 180 meV_{FWHM}

The 10 fs timescale is sufficient to resolve bond breaking and formation processes, vibrational dynamics, and most charge transfer processes (e.g., in materials and chemical systems). Furthermore, 10 fs time resolution is readily achievable with visible laser pulses (consisting of only a few optical cycles) which are used to drive much of the photochemistry of interest. At the same time, a Fourier transform resolution of 180 meV is sufficient to resolve relevant near-edge features (e.g. for absorption spectroscopy or resonant scattering) which are defined by core-hole lifetime broadening to be >200 meV typically.

High spectral resolution: 60 fs_{FWHM} ⇔ 30 meV_{FWHM}

Energy resolution at the 20-30 meV scale is sufficient to resolve a wide range of low-energy collective modes in correlated materials (e.g., typical energy gap for unconventional superconductors is ~50 meV), and can further resolve many relevant vibrational modes (e.g., metal-ligand stretch) in molecules. Note

that spectroscopy methods such as resonant inelastic X-ray scattering (RIXS) are not limited by the core-hole lifetime. Simultaneous Fourier-transform-limited time resolution at the 60 fs scale enables one to follow the evolution of collective modes in response to specific external perturbations (e.g., resonant vibrational excitation of materials, or charge-transfer excitations in molecules).

Extreme time resolution and large coherent bandwidth

Important applications in nonlinear X-ray science (particularly impulsive stimulated Raman for the generation of electronic wavepackets) will require <1 fs time resolution with large coherent bandwidth (3-5 eV) near the Fourier transform limit.

Spectral Range of Interest

The most important range of interest for soft X-rays (280 eV to 1 keV) is defined by the absorption edges of earth-abundant elements that are critical components of most chemical compounds, biological macromolecules, metallo-enzymes, and functional materials:

- C (284 eV), N (410 eV), O (543 eV)
- 3*d* transition-metal L-edges:
  Ti (454 eV), Cr (574 eV), Mn (639 eV), Fe (707 eV),
  Co (778 eV), Ni (853 eV), Cu (933 eV), Zn (1,022 eV)

Maximum Allowable Spectral "Pedestal"

In addition to the basic seeding criteria (e.g., ph/s/meV, narrow coherent BW), an important consideration in assessing seeding schemes is the expected integrated energy in any spectral pedestal (J_P) surrounding the narrow seeded line and how this pedestal energy compares to the total integrated pulse energy (J_0). This is important for spectroscopy applications, as the photons that contribute to a broad spectral pedestal can degrade the spectroscopy signals of interest. This depends on specific applications (and the detailed spectral characteristics of the pedestal), but we can define a simple benchmark: $J_P \sim J_0/2$, at which point, the shot-noise-limited signal/noise ratio degrades by a factor of $\sqrt{2}$. This is a very rough benchmark, and some applications will be more (or less) forgiving. In addition, there is always the option to use a monochromator to clean up the spectrum, but at a typical penalty (in terms of throughput efficiency) of ~0.1.

There are important potential practical benefits that arise from seeding:

- Higher average spectral flux (ph/s/meV) since a seeded XFEL delivers most of the power in the spectral bandwidth of interest, and minimizes any losses from post-XFEL spectral filtering.
- Timing synchronization from external seeding with short laser pulses may achieve higher performance (time resolution) by effectively eliminating the contribution from e-bunch timing jitter.
- Improved amplitude stability from a seeded XFEL (near saturation) compared with a SASE XFEL filtered with a monochromator.

The following are some of the key science areas (and the most relevant experimental approaches) for which seeded XFEL sources are expected to provide a qualitative advance:

Fundamental Dynamics of Energy & Charge

Charge migration, redistribution and localization, even in simple molecules, are not well understood at the quantum level. These processes are central to complex processes such as photosynthesis, catalysis, and bond formation/dissolution that govern all chemical reactions. Indirect evidence points to the importance of quantum coherences and coupled evolution of electronic and nuclear wavefunctions in many molecular

systems. However, we have not been able to directly observe these processes to date, and they are beyond the description of conventional chemistry models. High-repetition-rate soft X-rays from LCLS-II will enable new dynamic molecular reaction microscope techniques that will directly map charge distributions and reaction dynamics in the molecular frame. New nonlinear X-ray spectroscopies offer the potential to map quantum coherences in an element-specific way for the first time.

Experimental Approaches:

- Dynamic molecular reaction microscope
- Time-resolved photoemission spectroscopy
- Time-resolved hard X-ray scattering
- New nonlinear X-ray spectroscopies

Catalysis & Photo-catalysis

Understanding catalysis and photo-catalysis is essential for directed design of new systems for chemical transformation and solar energy conversion that are efficient, chemically selective, robust, and based on earth-abundant elements. LCLS-II will reveal the critical (and often rare) transient events in these multistep processes, from light harvesting, to charge separation, to charge migration and subsequent accumulation at catalytically active sites. Time-resolved, high-sensitivity, element-specific spectroscopy enabled by LCLS-II will provide the first direct view of charge dynamics and chemical processes at interfaces, making it possible to pinpoint where charge carriers are lost (within a molecular complex or device) — a crucial bottleneck for efficient solar energy conversion. Such approaches will capture rare chemical events in operating catalytic systems across multiple time and length scales. The unique LCLS-II capability for simultaneous delivery of hard and soft X-ray pulses opens the possibility to follow chemical dynamics (via spectroscopy), concurrent with structural dynamics (substrate scattering) during heterogeneous catalysis.

Experimental Approaches:

- Time-resolved resonant inelastic X-ray scattering and absorption spectroscopy
- Time-resolved X-ray photoelectron spectroscopy
- Simultaneous soft X-rays (spectroscopy) and hard X-rays (scattering)
- X-ray photon correlation spectroscopy
- New nonlinear X-ray spectroscopies

Emergent Phenomena in Quantum Materials

There is an urgent technology need to understand and then ultimately control the exotic properties of new materials – ranging from superconductivity to ferroelectricity to magnetism. These properties emerge from the correlated interactions of the constituent matter components of charge, spin, and phonons, and are not well described by conventional band models that underpin present semiconductor technologies. Fully coherent X-rays from LCLS-II will enable new high-resolution spectroscopy approaches that will map the collective excitations that define these new materials in unprecedented detail. Ultrashort X-ray pulses and optical fields will facilitate new coherent light-matter approaches for manipulating charge, spin, and phonon modes to both advance our fundamental understanding and point the way to new approaches for materials control.

Experimental Approaches:

- Time-resolved and high-resolution resonant inelastic X-ray scattering
- Time-resolved X-ray dichroism and coherent scattering/imaging
- Time- and spin-resolved hard X-ray photoemission

- X-ray photon correlation spectroscopy

New nonlinear X-ray spectroscopies refers to a broad class of new methods that exploit coherent X‑ray/matter interactions and incorporate sequences of X-ray pulses to generate experimental signals that are a function of multiple time delays and/or photon energies. In these techniques, X-rays are used both as a pump, to prepare element-specific non-equilibrium states of matter and as a probe of the time-evolution of these non-stationary states. As these tools rely on both ultrafast time resolution and resonant excitation, the ability to trade off pulse duration (<1 fs to ~100 fs) against bandwidth (>2 eV to ~20 meV) near the Fourier transform limit is very important. These tools further rely on the simultaneous combination of high peak power, high average power, tunability, and some degree of temporal and/or spatial coherence.

Experimental Approach	Res. Pwr.	Pulse Duration	Energy (eV)	SASE	mono	Self-Seeding	mono	Ext. Seeding	mono	comments
time-resolved spec. soft XAS, XMCD, PES	5,000	10-100 fs	250-1,000	maybe (1,2)	yes	maybe (2,3)	maybe (3)	yes (3,4)	maybe (3)	Spectroscopy near FT-limit R=5,000 (200 meV, 10 fs) Roughly core-hole lifetime limit
time-resolved spec. soft XES		10-100 fs	250-1,000	yes (2)	not needed	not needed	not needed	maybe (4)	not needed	X-ray excitation above absorption edge (non-resonant)
RIXS (hi-res, time-resolved) (also tr-ARPES)	5,000 50,000	10 fs 100 fs	250-1,000	maybe (1,2)	yes	maybe (1,2,3)	maybe (3)	yes (3,4)	maybe (3)	Spectroscopy near FT-limit: R=5,000 (200 meV, 10 fs) R=50,000 (20 meV, 100 fs) Requires max. ph/meV/pulse
time-resolved reaction microscope	5,000	10-100 fs	250-1,000	no (1)	N/A	maybe (1,2,3)	maybe (3)	yes (3,4)	maybe (3)	Spectroscopy near FT-limit: R=5,000 (200 meV, 10 fs) Roughly core-hole lifetime limit Target resonant chemical spectral features
Ultrafast, nonlinear, strong field	<500	<1 fs	250-1,000	no (5)	N/A	no (1,2)	N/A	yes (4,6)	no	Max. peak power and large coh. BW (~4 eV, 2 fs) for nonlinear Pulse duration less than core-hole lifetime (<5 fs) Ideally close to FT-limit, or non-spiked intensity profile to intrepret nonlinear effects
Ultrafast, nonlinear, strong field (resonant)	~2,000 (~500 meV)	5-15 fs	250-1,000	no (5)	N/A	no (1,2)	N/A	yes (4,6)	no	Max. peak power with some BW control to target resonances Pulse duration less than core-hole lifetime (<5 fs) Ideally close to FT-limit, or non-spiked intensity profile to intrepret nonlinear effects

yes = defiitely would be useful, or needed (depending on performance details)

maybe = might be useful, or somewhat useful (depending on performance details)

no = will not meet the needs for the technique or science

(1) spec. near FT-limit requires some BW and pulse-duration control

(2) requires some control of pulse duration near FT-limit (e-bunch duration, emittance spoiler etc.)

(3) pedestal may be an issue (or mono may be needed to filter spectral pedestal)

(4) additional potential benefit for synchronization (and stability?)

(5) requires single pulse (multiple time spikes are problematic)

(6) e-beam manipulation - e.g. eSASE (enhanced peak current), emittance spoiler etc.

Figure 3: Experimental approaches and requirements for the 250-1000 keV regime. This matrix identifies and summarizes the most compelling new experimental techniques (time-resolved XAS,RIXS, etc) and specifies how different lasing/seeding techniques meet these needs.

Seeding Techniques

Many seeding methods have been proposed to produce transform-limited pulses down to soft x-ray photon energies. Based on the criteria of performance, scientific impact, technical feasibility and maturity, beam quality requirements, R&D requirements, and risk evaluation, three schemes were identified for dedicated evaluation as candidates for LCLS-II seeding: SXRSS, Cascaded HGHG, and EEHG. Details are given in the following sections.

Leading Schemes

The different layouts of the leading seeding techniques for LCLS-II are illustrated in Figure 4.

Self-seeding is a straightforward extension to SASE FELs that can significantly increase the temporal coherence and spectral brilliance. It is also the simplest scheme to implement. Experimental demonstrations both of hard x-ray and soft x-ray self-seeding (HXRSS and SXRSS, respectively) at the LCLS have been carried out recently [J. Amann, et al, Nature Photonics 6, 693–698 (2012), D. Ratner et al. Phys. Rev. Lett. 114, 054801 (2015)], and these techniques have been used in user experiments. Self-seeding relies on the monochromatization and reinjection of the FEL radiation pulse partway through the amplification process using either crystals (HXRSS) or gratings (SXRSS) to select only a narrow region of the spectrum for gain. While capable of improving the spectral brightness by a factor of up to 50, such technologies may not be transferrable to high repetition rate machines (>10 kHz) due to optics damage constraints unless a robust cooling system is developed. The spectra produced from these schemes also show a shot-to-shot varying spectral "pedestal" due to a spectral mixing effect associated with long (e.g., ~1-5 micron) wavelength, non-ideal structures in the electron beam phase space. Such structures can arise from the microbunching instability (MBI), coherent synchrotron radiation (CSR) or wakefields. Elimination of such a pedestal could require the additional use of a downstream monochromator that would reduce the overall spectral brightness improvement to 2-5 times SASE.

To circumvent the need for high rep-rate survivable monochromators, the coherent FEL seed can be produced by a density modulation (bunching) in the electron beam. This is the principle of the high-gain harmonic generation (HGHG) technique, which uses a seed laser (typically UV wavelength) to modulate the electron beam energy in a short (few meter) undulator. The energy modulation develops into a density modulation containing high harmonics after passage through a dispersive chicane. In the FEL radiator, the beam radiates and amplifies coherent light at a harmonic of the laser wavelength. This is the method by which the FERMI FEL-1 produces coherent pulses from a 266 nm laser in the 100-20 nm wavelength regime. External laser seeding also enables significant control over the character of the FEL output. Recent efforts at FERMI have demonstrated various advanced options for coherent control over FEL parameters such as wavelength, bandwidth and pulse length, polarization, twin phase-locked pulses with tunable time or wavelength separation, simultaneous pulses with large (>10%) wavelength separation, and tunable FEL phase and chirp.

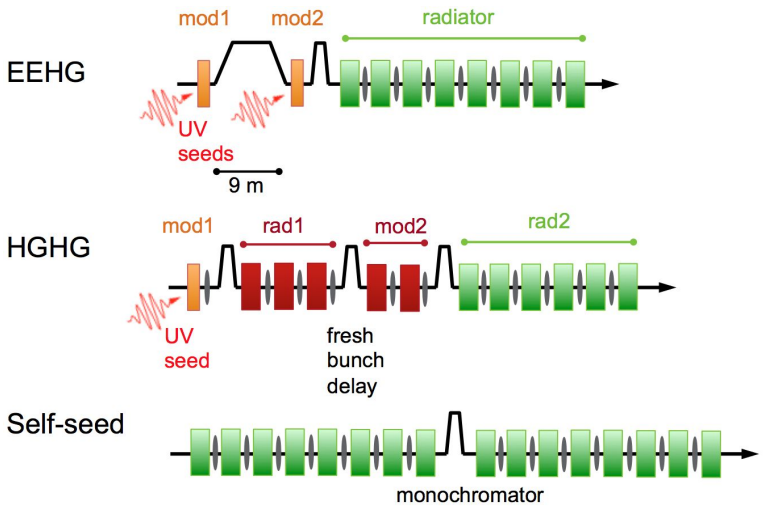

Figure 3: Seeding schemes and layouts for up to 1.24 keV soft x-ray energies.

While straightforward and versatile, the classical HGHG scheme has limited frequency up-conversion efficiency because generation of the harmonic h requires the laser energy modulation to be roughly h times larger than the beam slice energy spread. However, in order not to significantly degrade the FEL gain, the relative energy modulation also needs to be smaller than the normalized FEL bandwidth $\rho \sim 10^{-4}$ to 10^{-3}. This typically limits the harmonic numbers used in the classic HGHG scheme to less than $h \sim 15$. Thus, in order to generate coherent soft x-rays, multiple HGHG stages are needed (i.e., cascading), with each stage seeding a fresh temporal region of the electron beam. As a technologically challenging alternative, a sufficiently coherent and stable MW-class laser source at ~15 nm would enable access to 1 nm wavelengths in a single stage.

The frequency multiplication efficiency can be greatly improved with the echo-enabled harmonic generation (EEHG) technique. In this scheme, the laser energy modulation is followed by a strong chicane that filaments the phase space into energy bands, each with a width much smaller than the initial energy spread. A second laser then modulates the beam and, after passing through a second chicane, high harmonic bunching is produced. The key advantage of EEHG over HGHG is that by trading the large laser energy modulation with a large momentum compaction from a chicane, high harmonics can be generated from a relatively small energy modulation. This enables, in principle, the generation of high power, coherent soft x-rays directly from a UV seed laser in a single stage. The whole electron beam can be coherently bunched (rather than only a portion as in fresh bunch) to obtain longer FEL pulses and in principle much narrower bandwidths.

Other Concepts

Another proposed seeding option, high harmonic generation (HHG), is not considered a viable option for LCLS-II at present. HHG is a technique to produce sub-200 nm wavelength pulses by using a high power IR laser injected into a noble gas [A. McPherson, J. Opt. Soc. Am. B 4, 595 (1987)]. Direct HHG seeding of an FEL has been demonstrated from 160 nm wavelength down to 38 nm [G. Lambert, Nature Physics, 4, 296 (2008)., T. Togashi et al, Opt. Express 19, 317 (2011)., S. Ackermann et al. Phys. Rev. Lett. 111, 114801 (2013)], but the technique is currently limited to wavelengths above ~20 nm due to poor (<1e-6) harmonic conversion efficiency at shorter wavelengths. Below this point, the HHG seed does not have the required ~100 kW of power to dominate the FEL shot noise, unless petawatt-scale lasers are used [B.

Dromey et al., Nature Physics **2**, 456 - 459 (2006)]. Even so, the demonstrated resolving powers of the HHG pulse are only a few hundred, though this does not appear to be a fundamental limitation, especially if one considers HHG from solids [S. Ghimire, et al., Nature Physics 7, 138–141 (2011)]. Nevertheless, while there has been some progress by the laser community in extending high power HHG to shorter wavelengths, direct FEL seeding with HHG at x-ray wavelengths still requires a major advancement to achieve the necessary tunable (10-100 fs), high spectral brightness, high rep rate and stable pulses. As suggested above, the future availability of such pulses in the ~15 nm range could renew laser-driven HHG as a potential seeding candidate for soft x-ray FELs, possibly as an external driver for an HGHG configuration.

Coherent Inverse Compton Scattering (ICS) is a proposed concept to produce short wavelength radiation by scattering a laser off a low energy pre-bunched electron beam. The $\lambda = \lambda_L/4\gamma^2$ scaling shows that for $\lambda_L \sim 1-10\,\mu m$ laser wavelengths, the electron beam energy must be very low (<30 MeV) to reach 1 nm. To longitudinally pre-bunch the low energy beam at 1 nm, a concept that combines electron diffraction with emittance exchange has been suggested [E. A. Nanni, et al, arXiv:1506.07053 (2015)], and proof-of-principle experiments are currently being pursued. While the concept suggests a relatively compact x-ray source, there are several key technological challenges, particularly if ICS is to become a viable candidate for FEL seeding. For example, the method requires the production and transport of electron beams with transverse emittances of a few nm-rad together with sufficient longitudinal brightness and bunch length (>10s of fs) to produce the necessary narrowband, high peak power x-rays.

Performance Goals

The expectation for any seeding scheme in LCLS-II is the production of temporally coherent pulses with sufficient spectral brightness in the 1-4 nm regime to address the photon science requirements outlined in the matrix in Figure 3. These requirements include several features that favor a seeded FEL with many characteristics inherent to optical laser systems:

- *Enhanced Control:* Externally seeded FELs offer precise control of the central wavelength within a range much narrower than the SASE bandwidth, as well as the ability to control the coherent bandwidth either by seeding only a portion of the electron beam or by fully seeding beams of adjustable length. With coherent relative bandwidths potentially down below the 10^{-4} level, such flexibility with different realistic beams is a topic of ongoing study. Dedicated laser R&D is also needed to determine practical operational issues such as demands for high repetition rate modes, fast frequency dithering, and fine spectral phase control and feedback.

- *Frequency/Bandwidth Stability:* Seeding provides enhanced frequency and linewidth stability compared to SASE. In principle, the output frequency and bandwidth can be precisely set by the phase profile of the external seed lasers, as has been demonstrated at FERMI. Such control over stability may be possible with self-seeding or EEHG at LCLS-II. The impact and mitigation of resistive wall wakefield effects, which can introduce extra bandwidth into the FEL output pulse, is under active study.

- *Minimal Spectral Pedestal:* Longitudinal microbunching is predicted to be a significant effect at the LCLS-II due to the low gradient SCRF gun, relatively low energy of the 4 GeV beam, and the long transport system that brings the beam from the end of the SCRF linac to the Undulator Hall. MBI effects have been observed at LCLS when operating around 4 GeV despite the much shorter beam transport (<1 km), and are believed to be responsible for significant degradation of the

SXRSS performance [D. Ratner, et al. Phys. Rev. Lett. 114, 054801 (2015), D. Ratner, et al. Phys. Rev. ST Accel. Beams 18, 030704 (2015), Z. Zhang, et al. Phys. Rev. ST Accel. Beams 19, 050701 (2016)]. Similar degradation due to microbunching is suspected in the HGHG seeding experiments at FLASH [J. Boedewadt, IPAC'15]. Recent studies indicate that EEHG is less sensitive to longitudinal phase space structures because the strong dispersion introduces an inherent damping of the spectral pedestal, particularly as compared to HGHG [E. Hemsing, et al, Phys. Rev. ST Accel. Beams 20, 060702 (2017). Numerical simulations support that the EEHG spectral pedestal can be cleaner than the self-seeding spectrum for identical electron beams with a sufficiently high-quality longitudinal profile..

- *Coherent Two/Multi Color Operations:* Several different schemes to produce two-color x-ray pulses have recently been demonstrated at LCLS [A. A. Lutman et al., Phys. Rev. Lett. 110, 134801, (2013); A. Marinelli, Phys. Rev. Lett. 111, 134801 (2013); A. Marinelli et al., Nat. Comm, 6:6369, (2015)]. Depending on the technique used, the x-ray pulse energy separations can be varied up to a couple percent, and the timing delay up to a few tens of femtoseconds. Multiple colors are generally produced by lasing via the SASE process, but there are ways of seeding two colors at hard x-rays with the crystal monochromator [F. J. Decker et al., PRL, 113, 254801 (2014)]. However, such techniques would require additional hardware R&D beyond the baseline design of the soft-x-ray, self-seeding monochromator of LCLS and LCLS-II, and also must be compatible with the required repetition rates of LCLS-II.

  On the other hand, multicolor user experiments have been underway for several years at the FERMI FEL via the single stage HGHG configuration. At soft x-rays, EEHG may be used to seed coherent two-color operation by virtue of the closely spaced (by $1/h$) bunching harmonics, which could be amplified in LCLS-II using known split-undulator tuning arrangements. Also under study are methods to produce multiple phase-locked pulses using, for example, split and delay of the seed laser in the second EEHG seeding stage.

Start-to-End Beam Studies at LCLS-II

The IMPACT code was used to track both a 100 pC and a 300 pC electron beam (two standard configurations as of early 2017) from the cathode to the LCLS-II SXR undulator. The upper panels of Fig. 5 show the predicted longitudinal phase space of each beam. Note the apparent energy oscillations at short wavelengths developed from MBI growth, the curvature in the beam core, and the long tails. Figure 5 also shows the current profile of the head and core of each electron beam as well as the predicted time-dependent electron energy loss (in keV) per meter of distance travelled in the undulator (5 mm aperture) due to the resistive wall wakefield. These very long wavelength energy modulations can potentially broaden the bandwidth of a seeded FEL spectrum even in the absence of MBI-driven energy or density modulations. These beams are optimized primarily for low transverse emittance and high current, and are thus not necessarily optimized for seeding. Beams that are optimized better for seeding are currently under study.

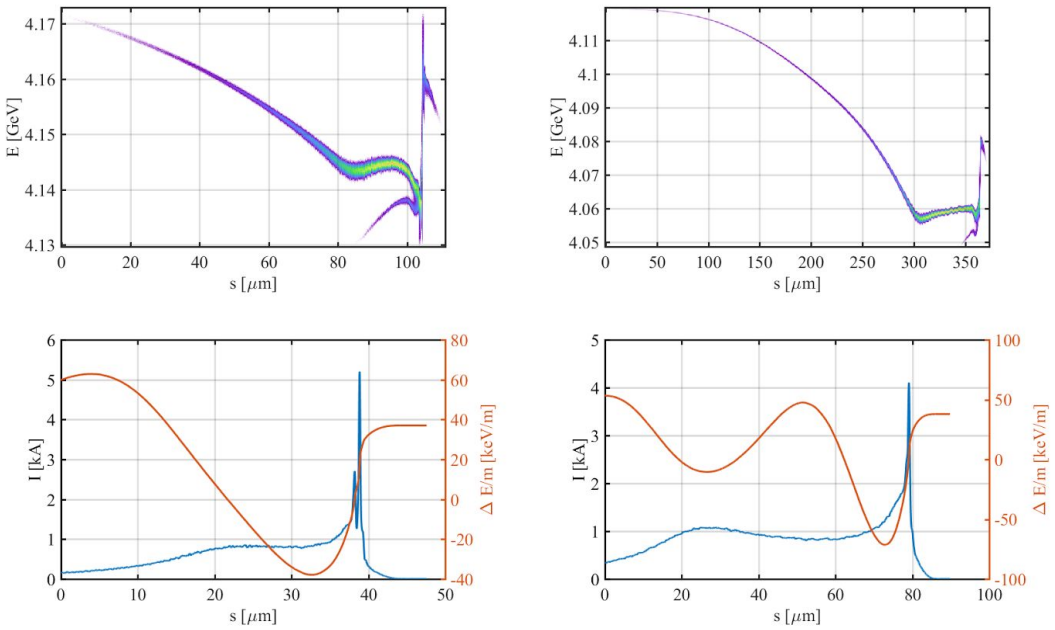

Figure 5. 100 pC and 300 pC electron beams from start-to-undulator IMPACT optimizations used for LCLS-II FEL simulations (head is to the right of the figures). Top left: Longitudinal phase space of 100 pC electron beam. Bottom Left: Current profile of the head and core of the 100 pC electron beam as well as the time-dependent energy loss per meter of distance in the undulator due to resistive wall wakefields. Top Right: Longitudinal phase space of 300 pC electron beam. Bottom Right: Current profile of the head and core of the 300 pC electron beam as well as the time-dependent energy loss per meter of distance in the undulator due to resistive wall wakefields.

Performance Comparison

Results of numerical simulations of Cascaded HGHG, EEHG, and Self-Seeding with the S2E beams and with ideal beams are shown in Figure 6. Also shown is the expected performance of monochromatized SASE. The laser-slicing XLEAP performance is also shown for comparison with an emerging short-pulse mode of operation.

The peak spectral density (photons/meV) is listed in the first row. The numbers indicate the value of the largest peak in the un-monochromatized output spectrum. As such, this captures the maximum spectral density of the raw FEL output available for post-monochromatization, independent of any accompanying spectral pedestal or noise. The addition of a monochromator would reduce the photons/meV according to the monochromator efficiency.

The spectral bandwidth of the FEL output is quantified in two different ways in order to capture the effect of the pedestal, which can have a complicated shape. The first way (second row of Fig. 6) computes the simple FWHM bandwidth of the most prominent spectral peak. The number of photons contained within this FWHM bandwidth, N_{fwhm}, is given in the third row as the percent fraction of the total number of photons, N.

Also given in the third row is the percent fraction of the photons contained in the pedestal. This pedestal fraction is calculated using a perfect gaussian spectrum as a benchmark, which contains 76% of the

photons in the FWHM central region, $N_{fwhm}/N=76\%$. Because the ideal gaussian is assumed to be pedestal-free, the spectral pedestal fractions from the simulations are calculated according to their departure from the gaussian ideal, namely, $f_{ped}=1-N_{fwhm}/0.76N$. This description can overestimate the pedestal for non-gaussian but idealized spectral distributions (e.g., a $sech^2$ function for which one would calculate $f_{ped}=7\%$), and can actually give negative pedestal fractions for spectra with sharp edges (i.e., waterbag distribution), but it provides some measure of simple relative comparison.

Accordingly, in the fourth row of Fig. 6 the "FWHM-equivalent" bandwidth ΔE_e is specified, which is the minimum spectral extent that contains 76% of the total pulse energy, E. This definition therefore incorporates the contribution of the pedestal, which can be overlooked by the more common FWHM definition. This distinction is useful, particularly for pedestals whose amplitude is less than half the seed peak height but that may contain a large fraction of the pulse energy. The "FWHM-equivalent" bandwidth seen in simulations is therefore generally much larger than the FWHM bandwidth, and may include more than one spectral spike, but it guarantees that 76% of the pulse energy is contained within.

The listed bandwidths and photon numbers are all calculated at the undulator position that gives the peak of the quantity $B_e=0.76E/\Delta E_e$ which is the number of photons contained within the relative FWHM-equivalent bandwidth. In each seeding scheme the pedestal tends to grow along the FEL undulator, so the resolving power $R=E/N\Delta E_e$ decreases even while the FEL pulse energy in the seeded spike increases exponentially. For example, the resolving power just downstream of the SXRSS monochromator may be very large (>10K), but the number of photons is small because the FEL has not amplified the seed appreciably (see Figs. 8 and 11). The maximum of B_e therefore algorithmically selects a location of peak dimensionless brightness that includes the FEL amplification and pedestal growth. In most cases, this location tends to be very close to saturation, but it moves downstream towards the end of the undulator when tapering is included. Tapering and wakefields are both included in all simulations.

There are many figures of merit that can be used to compare and judge the schemes, depending on the application. For example, the highest peak photon densities and B_e values are achieved with SXRSS (See Figure 6b), but the associated pedestals are typically larger than for EEHG. Overall, HGHG performs worst in terms of pedestal and photon density amongst the seeding schemes. The details and results are described in the following sections.

LCLS-II	Cascaded HGHG		EEHG		Self-Seeding		SASE+mono		XLEAP
	1 nm	2 nm	1 nm	2 nm	1 nm	2 nm	1 nm	2 nm	1-2 nm
Photons/meV/pulse (peak)	<1e8 3e7	1e9 4e8	2e10 2e9 7e8	3e11 5e9 8e9	7e10 4e10 1.7e10	6e11 2e11 1e11	4e9	2e10	5e9
FWHM (ΔE)	800 meV 400 meV	250 meV 400 meV	45 meV 170 meV 200 meV	60 meV 500 meV 200 meV	50 meV 80 meV 130 meV	50 meV 75 meV 90 meV	defined by mono	defined by mono	few eV
% of phot. in FWHM, % of phot. in pedestal	45%,40% 50%,35%	55%,30% 25%,70%	40%,50% 65%,15% 72%,5%	55%,30% 60%,20% 75%,1%	30%,55% 70%,10% 60%,20%	30%,60% 55%,30% 60%,20%	defined by mono	defined by mono	60%
FWHM-equivalent (ΔE_e)	SASE 1eV	SASE 1eV	200 meV 310 meV 250 meV	360 meV 900 meV 100 meV	620 meV 115 meV 205 meV	410 meV 180 meV 140 meV	defined by mono	defined by mono	few eV
pulse duration	10-20 fs	30 fs	15 -150 fs	10-150 fs	1-150 fs	1-150 fs	defined by mono	defined by mono	0.3-0.7 fs
Spectral Stability	med	med	high	high	high	high	best	best	low
Intensity Stability	low	med	med	med	high	high	med	med	med-high
Complexity	high	high	high	high	low-med	low-med	low	low	med
Two pulse/Multicolor?	no	no	yes	yes	yes/no	yes/no	yes/no	yes/no	maybe
Key: 300 pC S2E beam, 100 pC S2E beam, Ideal beam (50 fs, 1kA)									

Figure 6. Seeded LCLS-II performance comparison. The three different beams simulated are in different colors. In red are general expectations for general beams.

Beam	1 nm	2 nm
300 pC	1.28/0.10	7.2/3.4
100 pC	3.21/0.14	4.9/0.28
Ideal	0.36/0.07	2.6/1.1

Figure 6b: SXRSS/EEHG brightness comparison, $B_e=0.76E/\Delta E_e$ [1e16]. The highest peak photon densities and B_e values are achieved with SXRSS, but the associated pedestals are typically larger than for EEHG.

Soft X-Ray Self-Seeding (SXRSS)

LCLS SXRSS

Recent results from soft X-ray self-seeding (SXRSS) experiments at LCLS show an increase in peak brightness by a factor of 2-5 over SASE across the photon tuning range of 500-1000 eV with a measured resolving power of roughly 2000-5000. The persistent spectral pedestal, however, which when averaged over many shots, manifests itself as a small bandwidth of radiation about the resonant photon energy that is simultaneously amplified along with the seed. In Fig. 7 below we show some representative 1-keV self-seeding spectra taken recently at LCLS. By U18 (approximately 7 undulator sections beyond the self-seeding monochromator), at which point there is strong saturation, the mean integrated pedestal strength exceeds 20% of the amplified seed.

A leading explanation for this pedestal is long wavelength (i.e., 1-5 micron), small amplitude modulations on the energy and current of the electron beam produced by growth of the longitudinal microbunching instability upstream of the undulators [Z. Zhang, et al. Phys. Rev. ST Accel. Beams 19, 050701 (2016)]. The pedestal spectral contamination can be problematic for user experiments that require very narrow bandwidths with high spectral purity. While further downstream monochromatization is possible, the resultant cost in the reduction of soft x-ray photons can be substantial (i.e., > 10X). Therefore, significant effort has been devoted to understanding and eliminating the pedestal.

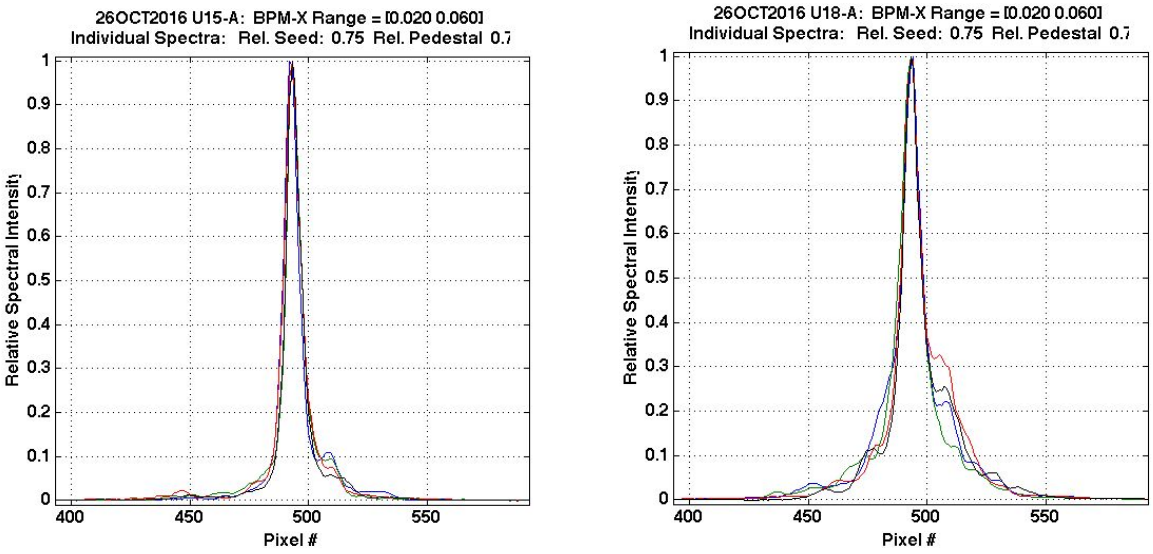

Figure 7. Self-seeding spectra taken at LCLS in October 2016 at 1 keV. The plot on the left shows data after the beam was deflected after U15 and on the right, after U18. The self-seeding monochromator is at U9 and U16 is effectively a drift. In each plot five individual spectra are selected whose amplified seed signal is in the 75th-percentile of all shots and whose pedestal strength is also at the 75th percentile. The grating resolution is 37 meV/pixel. These shots also lie in a narrow linac energy band corresponding to FEL resonance.

To study the expected magnitude of such pedestal formation, high fidelity numerical particle simulations using the ASTRA, ELEGANT, IMPACT and GENESIS codes have been used to evaluate the FEL performance of SXRSS for LCLS and LCLS-II in the presence of these energy modulations. For a given

excitation at the beginning of the injector, we have relatively high faith that the code ensembles give good accuracy concerning the predicted growth of the instability in the downstream linac for a given "tune". We also are reasonably confident in the predictions of the GENESIS FEL code, again for a given amplified excitation and set of electron beam properties at the undulator entrance. The key uncertainty is the actual excitation amplitude and spectrum in the LCLS-II injector, especially if there is any significant deviation from the "white noise" expected for simple stochastic shot noise. We note, however, that experimental studies on LCLS show that the measured microbunching level is in good quantitative accord with the predictions of the detailed simulation studies with the IMPACT code (see, e.g., Qiang et al., Phys. Rev. Accel. Beams **20**, 054402 (2017)).

LCLS-II SXRSS

300 pC SXRSS @ 1 nm

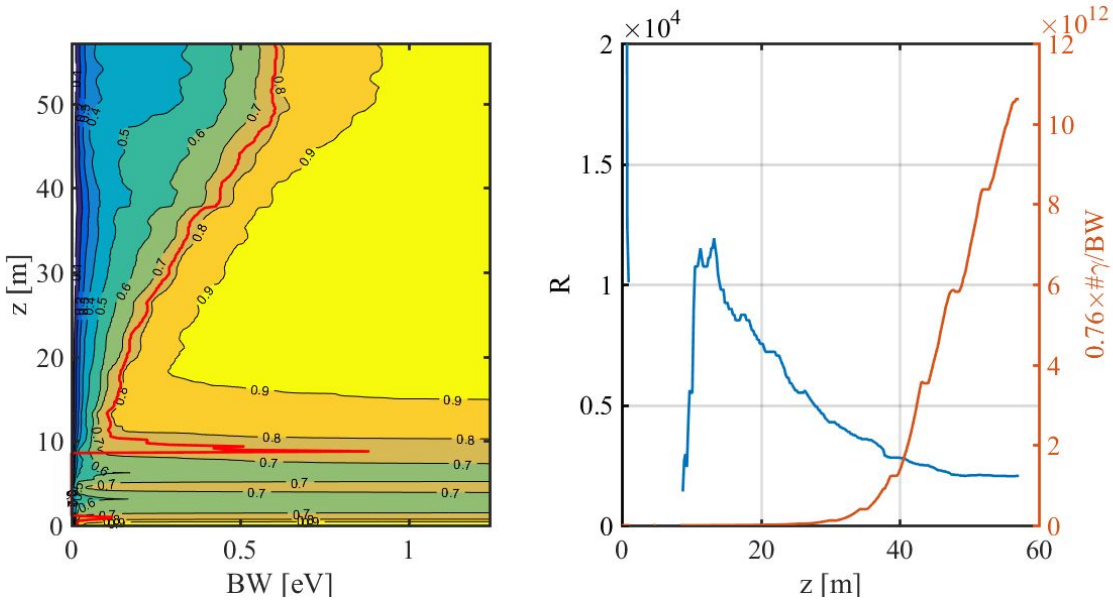

Figure 8. 300 pC LCLS-II beam SXRSS. Left: Fractional energy of the 1 nm (~1240 eV) seeded FEL pulse as a function of the distance along the undulator (vertical axis) and bandwidth about the seeded photon energy (horizontal axis). The red contour corresponds to a fractional energy of 76%. Right: Resolving power using the 76% fractional energy criterion (blue curve) and a measure of the spectral brightness B_e *(orange curve).*

The left panel of Figure 8 shows the fractional energy evolution for the FEL pulse along the undulator (after the SXRSS monochromator and chicane). Each contour indicates the fractional energy stored within a bandwidth about the seeded photon energy along the undulator. For instance, at z = 30 m, 76% of the photons exist within ~ 290 meV about the resonant photon energy. The positive correlation that exists between the distance along the undulator and the bandwidth for a given fractional energy indicates that wakefield- and MBI-driven energy and density modulations are decreasing the effective resolving power of the pulse. This is clearly indicated in the right panel of Figure 8, which shows the evolution of the resolving power along the seeded undulator using the 76% fractional energy criterion for the bandwidth calculation.

The increase in bandwidth of the seeded FEL is more clearly illustrated in the left panel of Figure 9, which shows the normalized spectral evolution along the undulator. The spectrum has a clear bifurcation

around z = 30 m, which is primarily due to the long wavelength energy modulation imprinted along the longitudinal profile of the electron beam from the resistive wall wakefield. The right panel of Figure 9 shows the spectrum at the peak of B_e (orange curve of the right panel of Figure 8) and shows a clear spectral splitting.

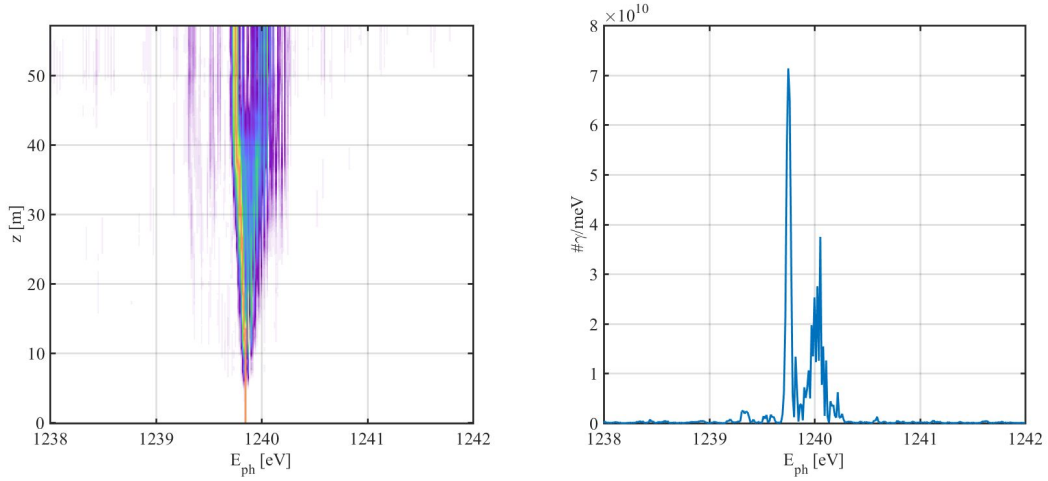

Figure 9. 300 pC LCLS-II beam SXRSS. Left: Normalized spectral evolution along the undulator. Right: Spectrum at the end of the undulator.

<u>300 pC SXRSS @ 2 nm</u>

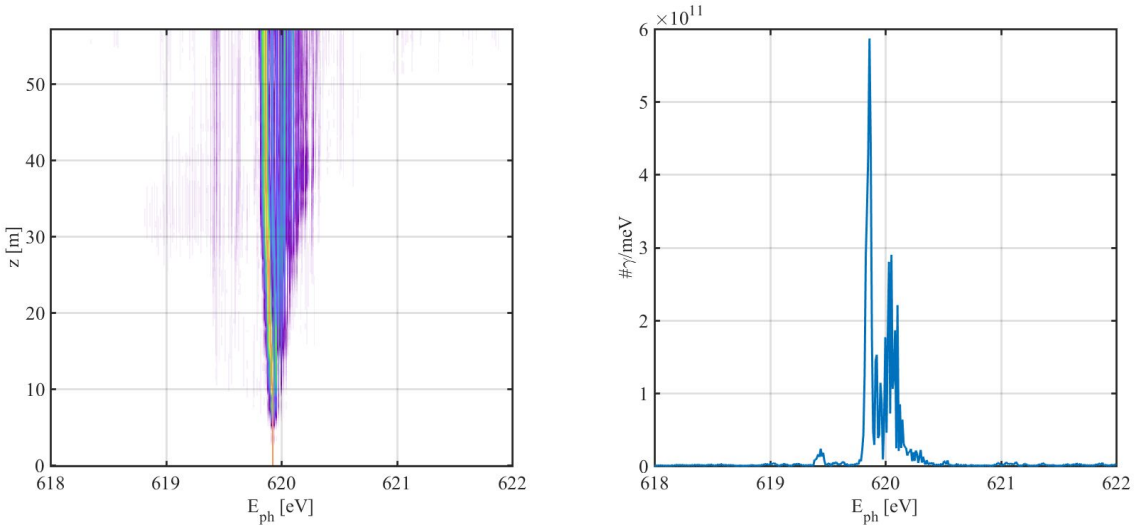

Figure 10. 300 pC LCLS-II beam SXRSS. Left: Normalized spectral evolution along the undulator. Right: Spectrum at the end of the undulator

The evolution of the fractional energy, resolving power, and spectral brightness for lasing at 2 nm with the 300 pC charge electron beam, given the 76% fractional energy criterion, is similar to the 1 nm case above. The MBI-induced energy modulations drive the amplification of pedestal photon energies. There is also a spectral bifurcation around z = 30 m in the seeded undulator, which is a result of the induced

time-dependent energy modulation from the resistive wall wakefield, as shown in the left panel of Figure 10. The spectrum at the peak of the spectral brightness (given the 76% fractional energy criterion) in the right panel of Figure 10 clearly shows this splitting.

100 pC SXRSS @ 1 nm

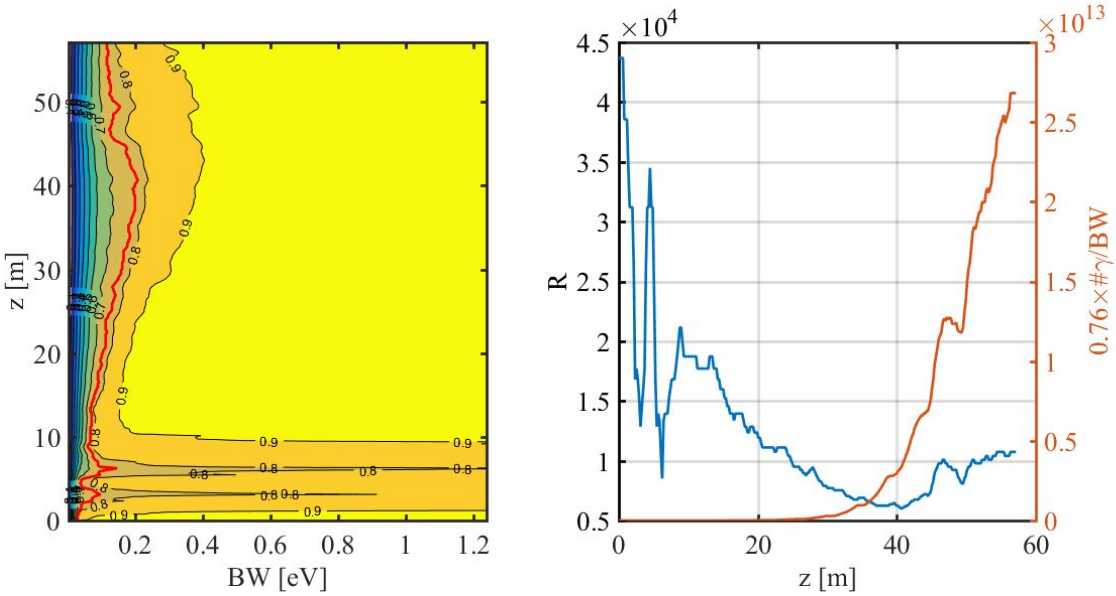

Figure 11. 100 pC LCLS-II beam SXRSS. Left: Fractional energy of the 1 nm (~1240 eV) seeded FEL pulse as a function of the distance along the undulator (vertical axis) and bandwidth about the seeded photon energy (horizontal axis). The red contour corresponds to a fractional energy of 76%. Right: Resolving power using the 76% fractional energy criterion (blue curve) and a measure of the spectral brightness (orange curve).

Recent SXRSS simulations for the 100 pC LCLS-II beam indicate a superior performance compared to the 300 pC case. The left panel of Figure 11 shows the fractional energy evolution along the seeded undulator. The 76% bandwidth contour does not indicate as dramatic a drop in resolving power that was seen from the 300 pC electron beam simulations. In fact, the tapered part of the undulator (the last 6 undulators or so) serves to increase the resolving power slightly, which can also be seen in the blue curve in the right panel of Figure 11. This is partially a consequence of the shorter temporal duration 100 pC electron beam (~50 fs), which is not as susceptible to resistive wall wakefield-driven bandwidth broadening. The cleaner spectrum is clearly seen in Figure 12. While MBI-driven modulations still serve to amplify frequency content in the spectral pedestal, the spectral splitting is not present.

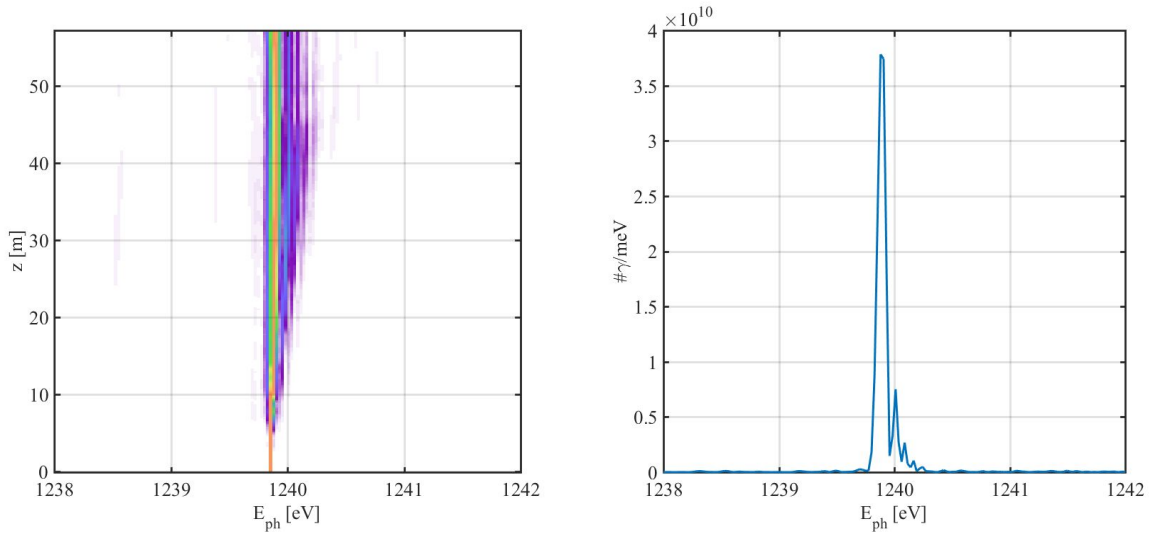

Figure 12. 100 pC LCLS-II beam SXRSS at 1 nm wavelength. Left: Normalized spectral evolution along the undulator. Right: Spectrum at the end of the undulator

It should be noted that the peak photon density (photons/meV) with the 100 pC electron beam at 1 nm is 50% of the value from the corresponding 1 nm simulation of the 300 pC beam, even though it has only one third of the charge. In addition, the resolving power is roughly 5 times greater and the brightness using the 76% fractional energy criterion is roughly 2.5 times greater for the 100 pC electron beam simulations.

100 pC SXRSS @ 2 nm

The behavior of the FEL and the evolution of the spectrum for the 100 pC electron beam at 2 nm is similar to the 1 nm case. The resistive wall wakefield does not drive significant spectral splitting, but MBI driven energy and density modulations continue to drive pedestal growth.

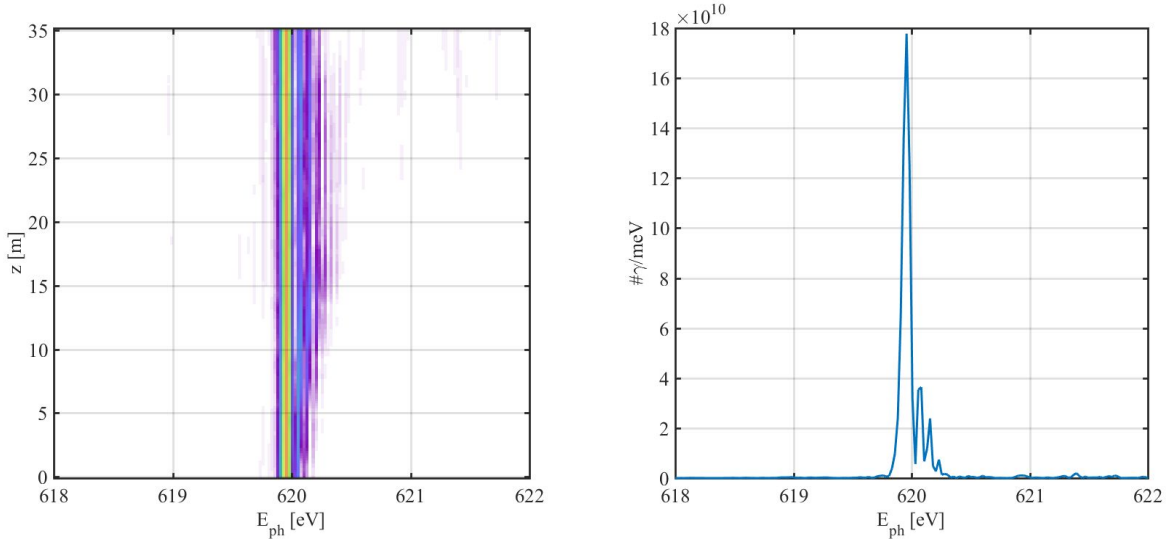

Figure 13. 100 pC LCLS-II beam SXRSS at 2 nm wavelength. Left: Normalized spectral evolution along the undulator. Right: Spectrum at the end of the undulator.

Issues for LCLS-II SXRSS

- *Spectral Purity:* As noted, the SXRSS spectrum is susceptible to pedestal formation and spectral splitting due to long wavelength electron beam phase space modulations. However, the lower charge 100 pC beam has a cleaner spectrum and higher peak brightness than the longer 300 pC beam due to the difference in wakefields experienced by the lower charge beam.

- *Mechanical Inflexibilities and Optical Coupling:* The LCLS-II SXRSS baseline deliverable involves repurposing the installed LCLS SXRSS system with only mechanical modifications to provide cooling to the optical elements for high power operation; whereas the layout and design specifications of the X-ray optics including the variable-line-spacing (VLS) monochromators, focusing mirrors and slits will remain unchanged. The properties of the LCLS-II SASE beam before the chicane including the effective source location and divergence will be different from those used for designing the LCLS system. As such, the coupling or overlapping of the electron and photon beams in the seeding undulator after the chicane was shown to be rather low and not optimized, certainly not over the energy tuning range from 200 to 1250 eV. The built-in mechanical rigidity of the LCLS system by having only one moveable element, i.e., the rotation of the VLS grating, does not enable significant optimization of the overall seeding performance. Compensating for the lack of flexibilities in the optical design by increasing the power of the SASE beam, i.e., adding additional undulators before the chicane, has been shown experimentally to enhance the quality of the seeded beam for the low-repetition rate LCLS system, but will be less viable for the LCLS-II high power operation due to the increase of the incident power on the optics. The lack of optical tuning capability of the LCLS system also may have degraded the seeding performance, especially in the limited gain in spectral brightness. These issues will remain for the LCLS-II system in the absence of a revised design, and are further complicated by potential thermal effects in the X-ray optics induced by the four orders of magnitude greater incident radiation power.

- *Heating of compact optical elements:* The footprint of the SASE beam on the VLS grating is significantly smaller (a few millimeters) than the typical scenario of a FEL output beam reflecting off a large mirror (hundreds of millimeters). As such, the cooling of the grating or focusing mirrors presents certain challenges. However, the planned LCLS-II SXRSS system will retain the LCLS optical design with a low resolving power of 5000, which entails several relaxed requirements on the mechanical specifications of the VLS grating and mirrors, such as slope error. Preliminary analysis assuming steady-state conditions indicates that with water cooling, the VLS grating would remain within specs for FEL repetition rates up to 100 kHz. If a much higher resolving power, for example, 50,000, were to be implemented, the cooling performance would have to be reassessed. Simple linear scaling would then put the maximum allowed repetition rate at 10 kHz.

Potential and Limitations

An improved SXRSS optical system for LCLS-II was designed that can produce a seed up to 30000 resolving power at 1.3 keV. At lower photon energies, the constraint for a transform-limited pulse would entail a lower resolving power, thus requiring a system with a more flexible optical design that provides a variable resolving power depending on the energy. These optical flexibilities can be realized only with greater mechanical complexities, including additional moveable degrees of freedoms. Specifically, tuning over large energy range would involve rotations of not only the VLS grating, but also a number of other optical elements. To tune over a small energy, say, a few eV, the variable resolving power system would

require only one simple rotation of the grating. More importantly, optimization of the seeding performance can now be pursued, and possibly achieved by matching the photon beam size with that of the electron beam by adjusting the imaging of the virtual source onto the immediate seeding undulator downstream of the chicane. The stability of a more mechanically complex system is of certain concern, but believed to be not out of reach. If the mitigation of the wakefield effect is not easily achievable, this becomes an ultimate limitation of the 4 GeV electron beam and then a moderate resolving power system, i.e., ~ 15000 at 1.3 keV, (i.e., referring to the 100 pC beam) should be considered. The required cooling performance will put a cap on the repetition rate at ~33 kHz. To go higher in repetition rate at 15000 resolving power, a cryogenic cooling scheme could be considered, albeit at a cost of an increasing amount of mechanical complexity.

Cascaded High Gain Harmonic Generation (HGHG)

In cascaded HGHG, the tail portion of the electron beam is coherently energy modulated by a laser (usually 260 nm wavelength), and the beam then transits through a dispersive chicane to produce harmonic bunching (e.g., h=13 at 20 nm). The microbunched beam is then sent into an undulator whose strength is tuned for resonant emission (and high gain) at the harmonic wavelength. The coherent FEL output then modulates the head of the beam after an electron beam delay section, and the process is repeated to reach much higher harmonics of the original seed wavelength (i.e., h=13x5=65 at 4.0 nm). This "fresh bunch" configuration together with a pulse shortening effect associated with high harmonics leads to an output radiation pulse much shorter than the full duration of the electron beam pulse. For a two-stage HGHG cascade operating at final harmonic 50 or higher, generally the output radiation pulse duration will be one-tenth or less than that of the electron beam.

The FERMI FEL-1 at Sincrotrone Trieste has been used as a single stage HGHG device to reach harmonics as high as 15 (17-nm wavelength) with peak powers of order 1-GW and energy fluences exceeding 100 microjoules [E. Allaria, et al., Nature Photonics 6, 699–704 (2012)]. The FEL-2 line is a two stage cascade and has reached the 4-nm "water window" with peak fluences of order 10 microjoules [E. Allaria, et al., Nature Photonics 7, 913–918 (2013)]. FERMI is currently operating as a user facility and has proved to be very attractive for experiments that require wavelength tunability, multicolor pulses, polarization tunability, and higher coherence than is generally available from SASE-based FELs.

The cascaded arrangement, however, places additional limitations on the pulse control and spectral brightness capabilities compared to single stage HGHG seeding, in part because the "fresh bunch" configuration limits the pulses that can fit within the optimal lasing core of the electron beam, and because non-ideal effects can be amplified by the intermediate stage. Combined, these issues result in expected performance issues with the LCLS-II beams, particularly the S2E beams that have strong energy distortions. As shown by the numbers listed in Figure 4, cascaded HGHG has the lowest photon spectral density and lowest resolving power (largest relative bandwidth) of the three seeding schemes at 1-2 nm. For these reasons, we presently believe that cascaded HGHG starting from a 260 nm laser is not a promising candidate for seeding LCLS-II at output wavelengths 2 nm and shorter..

Issues for Cascaded HGHG

- *Fresh Bunch:* Because the e-beam phase space is spoiled in each stage, cascading requires fresh bunch seeding which limits the maximum available resolving power as well as the peak brightness, since only a portion of the electrons can be used for the final stage FEL output. The

external seeding laser may be required to have a fast rise time in order to 'fit' into the seeded section of the electron bunch without increasing the energy spread in the fresh-bunch section. Simulations with super-gaussian seed laser temporal profiles on ideal beams, however, still exhibit multi-spiked spectra due to the growth of SASE in the adjacent portions of the beam.

- *Sensitivity to e-beam phase space structure:* For a high total harmonic jump, small modulations or irregularities in the electron beam longitudinal phase space can lead to strong phase and power variations in the output x-ray radiation pulse. In the 1-2 nm regime, the maximum tolerable size for energy modulations from instabilities is smaller than the predicted slice energy spread. A fluctuating linear energy chirp in the electron beam will lead to a fluctuation in the final wavelength at a level that is approximately 10-20 times that of EEHG, because the shift in wavelength is multiplied by the harmonic jump of the second stage.

- *Controlling output pulse length*: To reach the range of 1-2 nm wavelength in 2-stage HGHG, both stages must go to fairly high harmonic jumps of order 10. This makes it difficult to preserve contrast between the seeded radiation pulse and SASE radiation coming from unseeded portions of the bunch, especially if there are current spikes towards the head of the bunch. Slippage in the first modulating undulator can stretch the effective input pulse duration, but this is usually mitigated by the pulse shortening effect for high harmonics. As a result, pulse length control in cascaded HGHG is limited unless more elaborate two-bunch schemes are used.

- *Synchronization/jitter requirements*: Because the fresh head part of the bunch should not directly interact with the external laser, the delay chicane strength must be sufficient to delay the e-beam well beyond the rising portion of the external laser pulse (which modulates the tail portion). Moreover, slippage both in the first modulator and radiator undulators increase the effective length of the laser pulse. These effects lead to a need for an added buffer zone between the sections of the bunch corresponding to the two radiation stages. Finally, timing jitter between the laser and the electron bunch requires a further buffer at the tail of the electron beam bunch to ensure that the main part of the laser pulse fully falls on a useful electron bunch portion. All these effects reduce the maximum possible duration of the output FEL pulse from the second radiator for a given electron beam pulse length. As an experimental example, at FERMI the output radiation pulse duration for 2-stage HGHG is of order 50 fs or less despite an electron beam pulse length in general exceeding 500 fs. For LCLS-II with a much shorter expected electron beam pulse length, output durations would likely be 30 fs or less, and still suffer from SASE build up that can spoil the spectrum.

Short Wavelength, Single Stage HGHG Seeding

- Because some of the concerns for cascaded HGHG push one towards choosing a large initial energy modulation, it is worth revisiting the issue of whether single stage HGHG can be made to work. Using short-wavelength radiation sources could be an avenue towards reaching keV photon energies in this way, but so far experimental studies using HHG sources have shown this to be challenging (see above). Similarly, other schemes such as coherent ICS do not appear to be promising options as of yet, due to their relatively large bandwidths (>1%) and strict external electron beam source and transport requirements.

- Using a UV wavelength laser to reach soft x-rays in a single stage would require extremely large energy modulations, preventing FEL amplification of the electron bunching. This would limit the radiating undulator to a small number of periods and constrain the total photon flux. In this setup,

however, the FEL output is comprised of a pulse train rather than a single long pulse because the slippage is less than the laser wavelength [Garcia, Phys. Rev. Accel. Beams 19, 090701 (2016)]. There are other issues with such a scheme, such as the ability to yield sufficiently narrow current spikes in a beam modulated by such a large amount.

Potential and Limitations

Cascaded HGHG has a demonstrated potential to produce high harmonics of a single external laser, but the longitudinal phase space of the beam has a large impact on the maximum achievable harmonic. Reaching 2 nm wavelength x-ray pulses beginning with a UV laser already seems to be a challenge for a two-stage cascade. Short pulses where the spectral quality is not a pressing concern would be the most likely target for this scheme, at which point simpler e-beam slicing techniques may be preferable. Longer electron bunches could allow for a cascade with more than 2 stages, but this has not been demonstrated experimentally. The performance may be improved with the use of bunches with long duration, low peak current, low energy spread, minimal energy modulations, and that contain no current spikes. This would, however, lead to much longer gain lengths in the final radiator and reduced peak power (and likely total output radiation pulse energy as well).

Echo-Enabled Harmonic Generation (EEHG)

EEHG simulations have been performed using the LCLS-II S2E beam distributions. The system under study is chosen to fit within the ~40 m section upstream of the soft x-ray undulator in the hall (Figure 1), including a small laser injection chicane that can be added upstream (but is not modeled in simulations). Specifically, the simulated EEHG beamline begins with a 20 m section (the equivalent of 5 undulator slots) that contains two modulation stages, each followed by a chicane. This section is followed by the long FEL undulator where the coherently bunched beam radiates in the soft x-ray regime.

The EEHG parameters used in simulations are shown in Figure 14. These simulations use two 3.2 m long modulators tuned to be resonant with a 4 GeV beam at λ_L=260 nm, but they need not be identical. In fact, it is typically better for the second modulator to be weaker in strength to avoid IBS and space-charge effects that can have deleterious effects on the electron beam phase space. The 260 nm, GW-class seed lasers come to a waist in the middle of the modulators with 1 m Rayleigh lengths. Each of the four-dipole symmetric chicanes use magnets with identical fields and length, as well as drifts of identical length.

Element	Strength 1(2) nm	Length
Mod 1	K=25 ΔE=1.5 MeV (1 MeV)	3.2 m λ_u=10 cm
Mod 2	K=12.5 ΔE=3 MeV (2 MeV)	3.2 m λ_u=40 cm
Chic 1	R_{56}=14 mm (9.8 mm)	9.25 m L_m=2 m
Chic 2	R_{56}=53 μm (85 μm)	2.25 m L_m=25 cm

Figure 14. EEHG parameters used in LCLS-II simulations.

EEHG at 2 nm

Results are shown in Figure 15 for the 300 pC bunch. In these simulations, the two input lasers are taken to have the same wavelength and 400 fs pulse duration, but this is not essential. The effects of wake fields in the radiators are also included. Undulator tapering is used to optimize performance. Note the narrowing of the spectrum and suppression of the pedestal compared with the self seeded spectra in Figure 10. With EEHG the spectral spike contains a higher relative fraction of the total number of photons within the 60 meV FWHM bandwidth (55% compared to 30% with SXRSS), and the FWHM-equivalent bandwidth is narrower (360 meV compared to 410 meV) due to the smaller pedestal and lack of strong spectral splitting from resistive wakefields. However, the total number of coherent photons with EEHG is about 5 times less than with SXRSS, likely due in part to the increased energy spread (from the lasers), and to the deformation of the phase space from the strong dispersion.

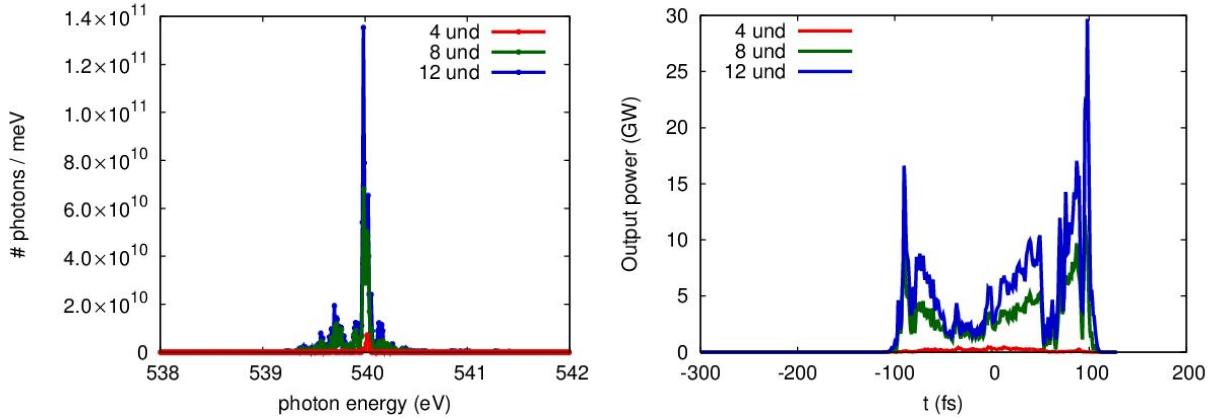

Figure 15. EEHG at 2.3 nm using a 300 pC electron beam from IMPACT simulations of LCLS-II and 400 fs FWHM lasers. Left: EEHG spectrum (single shot) at various positions in the beamline. Note the improvement in the spectral brightness and a strong suppression of the pedestal compared with the self-seeded results in Figure 10. Right: EEHG power profile at saturation (single shot). Tapering is not equally effective across the core of the bunch, but it does help to maintain the quality of the spectrum.

Other EEHG simulations were performed on the 300 pC LCLS-II beam using a variety of lasers and chicane configurations, with similar results. For temporally short seed lasers it is difficult to maintain good contrast against SASE from the unseeded portions of the bunch, similar to cascaded HGHG.

We see that in EEHG, the large shearing of the phase space during the manipulation process tends to reduce the impact of small initial energy variations in the beam (eg, MBI), which results in a somewhat cleaner spectrum compared to self-seeding with the 300 pC beam at 2 nm. This is because the large initial dispersion in EEHG acts like an effective damping for small modulations with wavelengths less than about $\pi R_{56}\sigma_{\delta} \cong 3$ μm, and because the two seeded energy modulations mix in a way that partially cancel the impact of initial energy offsets. There is usually a spectral pedestal even at the very beginning of the soft x-ray radiation stage, but its spectral width is typically smaller than observed for self-seeding simulations with the same S2E beam. However, for some combinations of electron bunch profile and dispersion in the EEHG section, the post dispersion section electron beam is significantly less optimal for clean radiation production than the original distribution. In particular, current spikes can be enhanced and the beam can fold over on itself, which leads to greater SASE background.

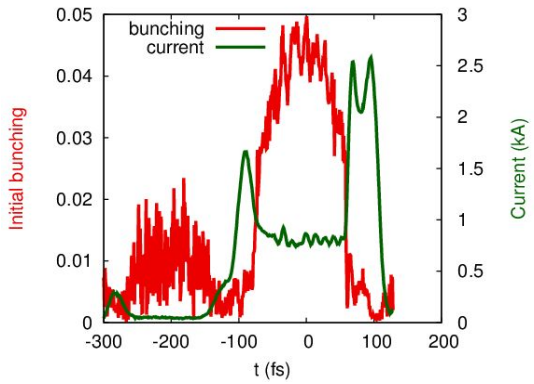

Figure 16. The bunching fraction at 2.3 nm produced through EEHG with the 300 pC beam is shown against the peak current profile after the first chicane.

EEHG at 1 nm

For output wavelengths down to 1 nm, there are two main complications that occur when compared to longer wavelengths. The first chicane has an even larger R_{56} which, while serving to suppress even longer wavelength small amplitude energy modulations, causes even greater bunch distortions for the large amplitude structures like the tails. This can produce current spikes and increase the slice energy spread. Another concern is that the induced energy spread from the required energy modulations must increase to reach higher harmonics, but at the same time the downstream FEL amplification at shorter wavelengths becomes more sensitive to the energy spread. For the beam quality that has been measured in LCLS and is predicted by simulations for LCLS-II, the gain length for the modulated beam can become roughly 50% longer than would be true for SASE in the absence of seeding. This increase requires more total undulator length to reach saturation, and can lead to a higher SASE background wherever the seed lasers do not temporally cover the electron bunch.

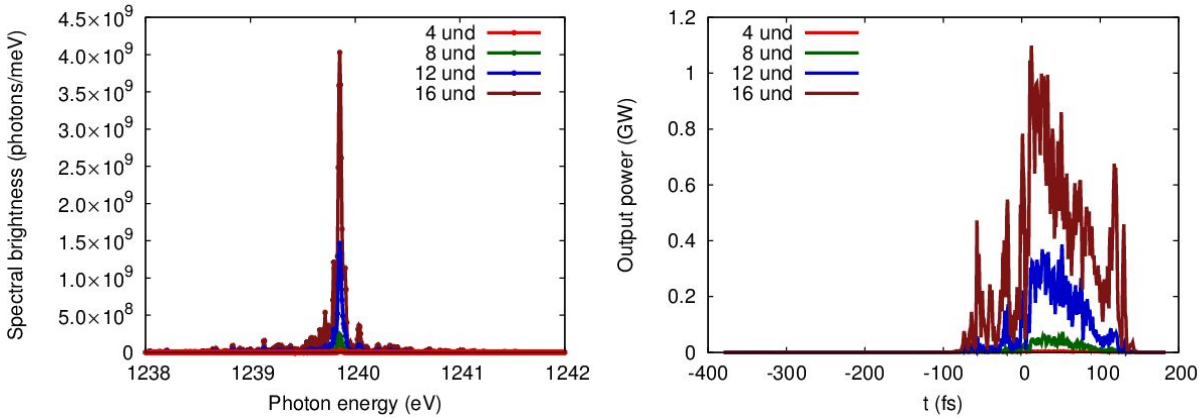

Figure 17. EEHG at 1 nm using a 300 pC electron beam from IMPACT simulations of LCLS-II and 400 fs FWHM seed lasers. Left: EEHG spectrum (single shot) at various positions in the beamline. Right: EEHG power profile at saturation (single shot). Compared with the self seeded LCLS-II case EEHG has reduced spectral brightness and produces a slightly narrower pedestal.

Figure 17 shows the spectrum and power profiles for the 300 pC bunch radiating at 1 nm. The spectrum has a pedestal which covers a slightly narrower spectral range than the 1 nm self-seeding example, and

again lacks the sideband components from the resistive wall wakefield. The gain length and final power, on the other hand, are noticeably degraded. The spectrum can be cleaned up by not going to saturation, but the pulse energy is reduced by a factor of three and the spectral brightness by a factor of two.

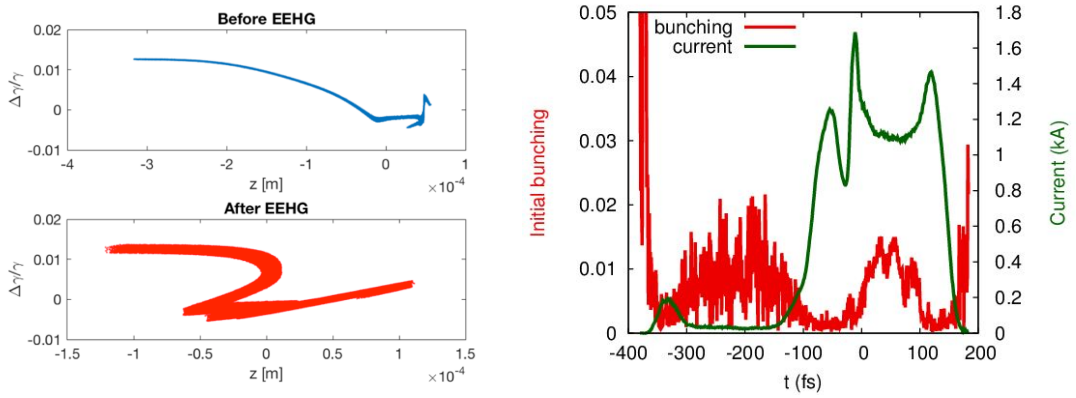

Figure 18. Left: Transformation of the 300 pC phase space with EEHG at 1 nm. Right: The bunching fraction at 1 nm produced via the EEHG process is shown against the peak current profile after the first chicane.

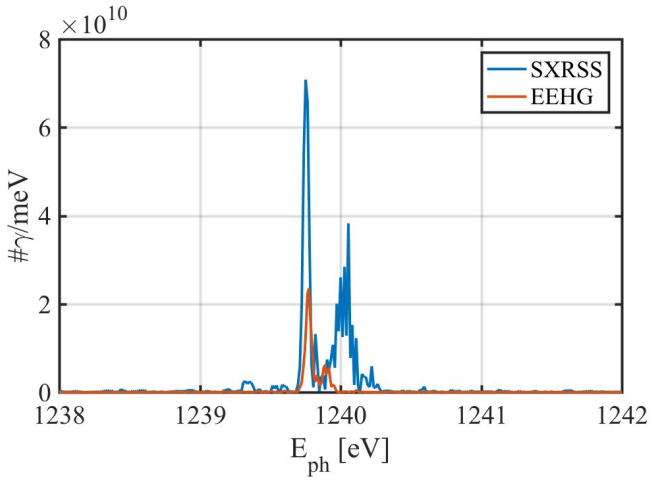

Figure 19. 300 pC beam output radiation spectra at 1 nm with SXRSS and EEHG.

100 pC Beam

The EEHG spectra and temporal pulse profiles from the shorter 100 pC beam are shown in Figure 20. At 1 nm, the FWHM of the spike is 170 meV, and contains 3e11 photons; a factor of 20 smaller spectral brightness than was produced by SXRSS simulations. While the radiation pulse is only about 3 times the transform limit for both EEHG and SXRSS, the factor of two larger bandwidth with EEHG is the result of the strong distortion of the longitudinal phase space that limits the lasing core to a shorter temporal

region.

At 2 nm, however, the EEHG spectrum has multiple 50 meV FWHM spikes separated by 90 meV that together cover 1 eV. These are the result of interference between the head and tail current spikes in the e-beam generated by the large dispersion that produce two temporally separated FEL pulses. This interference makes for a somewhat ill-defined definition of pedestal and performance. Such a feature may be useful for phase locked multicolor operations, but this arrangement does not readily produce a single spectral spike.

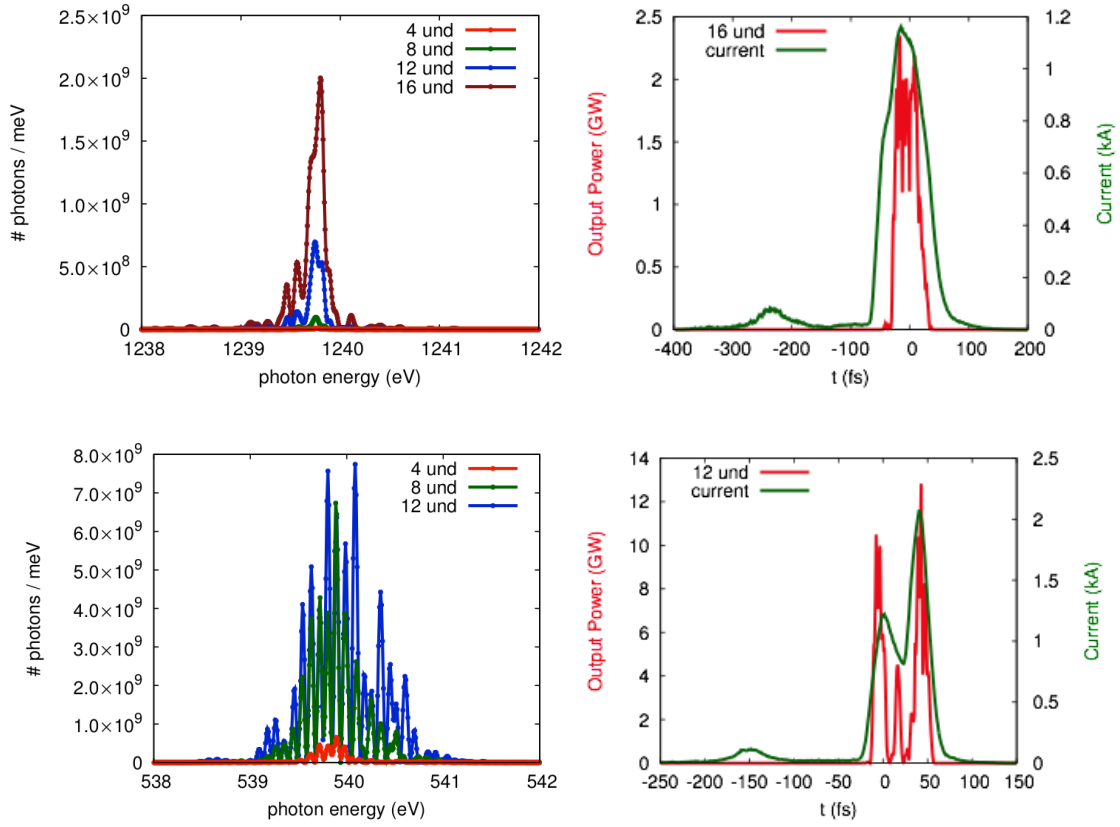

Figure 20. EEHG with the 100 pC S2E LCLS-II beam at 1 nm (top) and 2.3 nm (bottom).

Issues for EEHG

- *Laser Spectral Phase:* A significant issue present for all harmonic generation schemes, the eikonal phase of the input laser gets multiplied by the very large harmonic factor. For EEHG, this issue is most relevant for the second external laser pulse. This effect is somewhat suppressed by the large pulse shortening effect which reduces the impact of temporal phase deviations in the tails of the laser pulse. However, in the main body of the laser pulse, the phase wander may be required to be of order a couple degrees or less to reach soft x-ray wavelengths directly from the UV. With sufficient laser power in cases where short output radiation pulses are not wanted, however, it may be possible in EEHG to stretch the laser pulse such that the phase errors and corresponding laser chirp are within the required tolerances.

- *MBI Growth:* The coupling of the 260 nm laser with the 4 GeV beam requires undulators with periods on the order of tens of centimeters and correspondingly large strengths $K \leq 25$. The undulators increase the effect of longitudinal space charge in the beam, essentially because they act like an extra $1+K^2/2$ factor in drift length. For large K, and combined with the seeding chicanes, the MBI effects can be amplified and the phase space modified. Early estimates suggest that the integrated effect can be a reduction of up to 30% in the bunching magnitude, depending sensitively on the beam and lattice parameters. The long wavelength longitudinal space charge effect can also introduce energy structure in the beam as it propagates through the undulators, which can shift and/or compromise the coherence of the bunching, particularly in the second modulator. As is the case for energy scatter, any energy distortions which occur in or between the two chicanes will have a pronounced impact on the spectrum compared with distortions that occur elsewhere. We are presently examining this issue in detail.

- *ISR-driven energy spread growth*: The transit of the beam through the modulators also induces ISR. The second undulator is more constrained than the first because of the fine-grained energy structure in EEHG. The undulator period cannot be too short or the required high magnetic fields give too much scattering from ISR, which washes out the bunching at high harmonics. As such, the lattice should be designed (as it is in the simulations) so that scattering from both IBS and ISR in the modulators will not have major effect.

- *Other impacts of the large chicane*: The chicane after the first energy modulation has a very large dispersion that can substantially change the electron beam phase space and current profile. For example, the tail region, which tends to have higher electron energy than the main core of the bunch, can become compressed or even overlap the core (see Figure 18). A possible solution might be to design the first injection chicane to produce an equal but opposite dispersion to preempt the folding. Otherwise, energy modulations from long wavelength microbunching can be converted to substantial current fluctuations, which may also disrupt the coherence of the x-ray radiation. ISR and IBS from the chicanes can also impact the magnitude of the initial bunching, which at the 1 nm EEHG setting may be degraded by ~15%. Another potential issue is CSR, which can introduce uncompensated energy structures in the beam that can spoil the robustness of the spectrum. This is also a topic of active study.

Potential and Limitations

EEHG has a strong potential to provide long, coherent pulses as well as short or otherwise tailored x-ray pulses (*e.g.,* multiple pulses). However, due to energy scattering effects there are constraints on the maximum harmonic jump that is achievable in practice. Furthermore, the initial energy spread can be almost irrelevant in determining EEHG performance because of the dominant impact of energy scatter. For LCLS-II parameters, starting from a UV wavelength seed we believe that a photon energy of 1 keV is close to the maximum achievable using a single stage of EEHG because the required energy modulation becomes comparable to the total energy acceptance of the FEL. Avoiding this problem requires significant improvements in beam emittance, peak current, or undulator technology. Using shorter wavelengths for the second energy modulation would also improve performance.

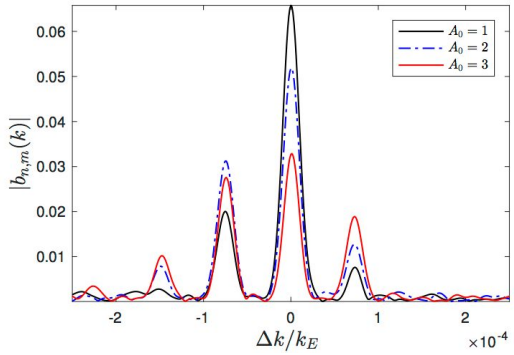

Figure 21. Multicolor seeding with EEHG is possible with an additional long wavelength modulation to produce bunching in sidebands.

Seeding the entire electron beam in EEHG is the most straightforward case to implement. Short regions within the electron bunch can be seeded but then competition with SASE from other parts of the bunch must be considered (we note that this issue is common to many of the seeding schemes).

The large chicane strength needed for EEHG does present novel challenges, but it may be possible to design the accelerator to use this final dispersive section to reach its optimal configuration. Lowering the overall microbunching gain in the linac may be more difficult to implement.

A compelling and unique feature of EEHG compared to SXRSS is the capability for coherent multicolor operations. EEHG naturally produces bunching at harmonics adjacent to the target harmonic, *h*. Therefore, using a split-undulator configuration to amplify one or more of these nearby frequencies, multicolor soft x-ray FEL operations are possible with color separations of 1/*h*. Alternately, for much smaller color separations, (eg, within the ~0.1% FEL bandwidth), a coherent energy modulation introduced on the beam upstream of the EEHG beamline with a wavelength of a few microns can produce bunching at closely positioned sidebands. Shown in Figure 21, such a scenario can be achieved with the XLEAP 2 μm laser, or potentially via beatwave modulations introduced at the upstream laser heater [E. Roussel, et al, Phys. Rev. Lett. 115, 21, 214801 (2015)].

Ideal Beams at LCLS-II

Given the much less than perfect seeding performance of the S2E beams, simulations with ideal, flat-top 1 kA current profile, 50 fs beams were performed to establish the baseline expectations of EEHG and SXRSS. Electron beams longer than 50 fs tend to perform worse for both schemes due to the resistive wall wakefields in the LCLS-II undulators, which add nonlinear structure to the otherwise ideal linear e-beam phase space that fragments the spectrum. For beams shorter than 50 fs, the effect of the wake is to introduce a nearly linear chirp in the FEL output.

SXRSS

The SXRSS photon seed is assumed to be ideal. The figures below correspond only to the seeded part of the undulator. The upstream SASE undulator, which nominally serves the purpose of generating the radiation to be monochromatized, is simulated to estimate the properties of the ideal seeded radiation used downstream as well as to capture the impact of the SASE process on the slice properties of the ideal

electron beam. The effects of resistive wall wakefields in the undulators are included throughout the simulation.

1nm

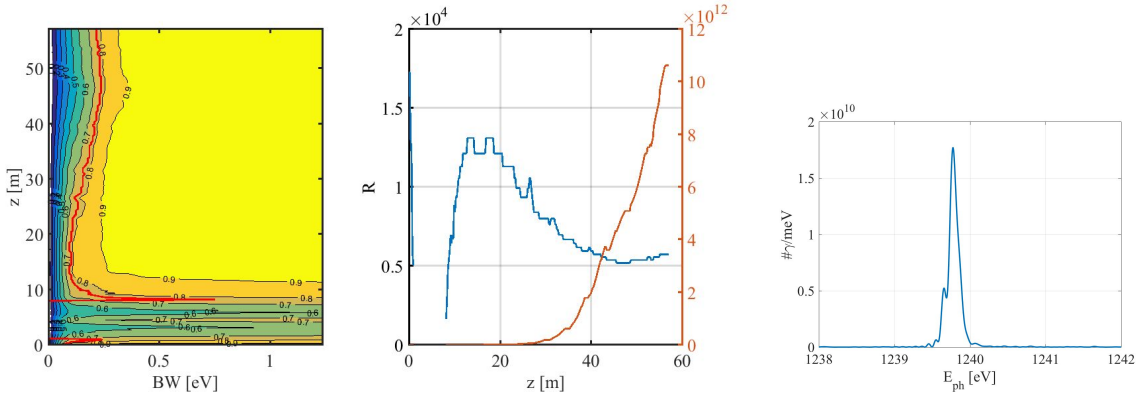

Figure 22. Ideal LCLS-II beams SXRSS at 1 nm (~1240 eV). Left: Fractional energy of the 1 nm seeded FEL pulse as a function of the distance along the undulator (vertical axis) and bandwidth about the seeded photon energy (horizontal axis). The red contour corresponds to a fractional energy of 76%. Center: Resolving power using the 76% fractional energy criterion (blue curve) and a measure of the spectral brightness (orange curve). Lower Left: Normalized spectral evolution along the undulator. Right: Spectrum at the end of the undulator.

The left panel of Figure 22 shows the fractional energy evolution for the FEL pulse along the undulator (after the SXRSS monochromator and chicane). A detailed description of these contour plots can be found in the start-to-end SXRSS section. There seems to be some bandwidth growth after ~20 m that is a consequence of the resistive wall wakefield induced energy chirp. This is clearly indicated in the evolution and steady reduction of the resolving power. This should be contrasted with S2E beam simulations that show bandwidth growth due to effects from the microbunching instability. The final output FEL spectrum is essentially a 130 meV FWHM single spike.

2 nm

The results for ideal simulations at 2 nm are shown in Figure 23. The evolution of the spectrum and the resolving power associated with the 76% fractional energy criteria are similar to the results for ideal simulations at 1 nm. The final output is essentially single spike with a minimal pedestal.

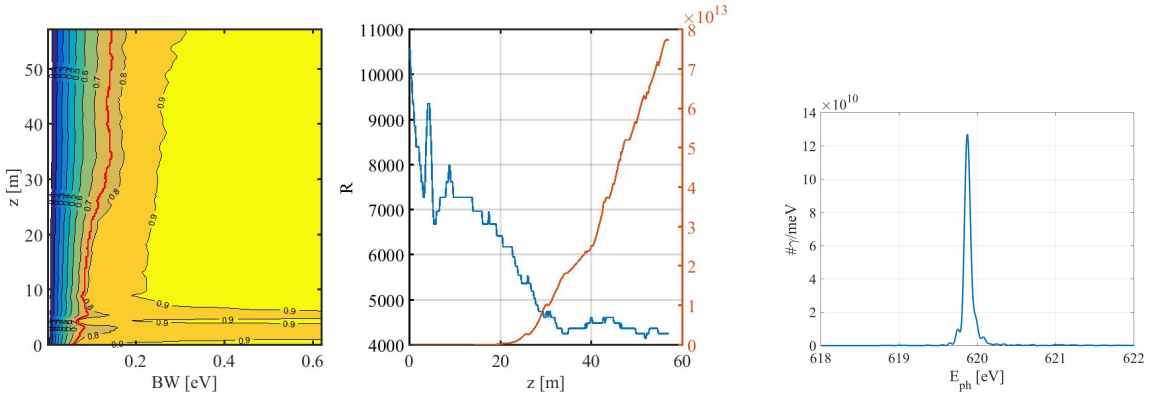

Figure 23. Ideal LCLS-II beams SXRSS at 2 nm (~620 eV). Left: Fractional energy of the seeded FEL pulse. Center: Resolving power and spectral brightness. Right: Spectrum at the end of the undulator.

Cascaded HGHG

We revisit cascaded HGHG employing the ideal short bunch (50 fs), flat-top current profile beam. To accommodate the fresh-bunch scheme and avoid increasing the energy spread everywhere in the first stage, the seed laser is taken to have a super-gaussian profile with a 20 fs FWHM. This would not be necessary for a longer electron bunch, but the beam would again be more strongly influenced by wakefields. While output pulses can be generated at these short 1-2 nm wavelengths, the spectrum tends to be broad with multiple peaks. The output pulse is also likely to be highly sensitive to shot-to-shot variations in the electron bunch, including fluctuations in the timing. Slippage within the first undulator is reduced compared to previous simulations by reducing the number of periods by a factor of four.

To produce radiation at 1 nm, the input laser at 260 nm is used to generate bunching at the intermediate wavelength of 13 nm. Radiation at 2 nm is obtained by setting the intermediate wavelength to 20 nm. In addition, the first radiating undulator tuned to 20 nm is turned off (the gap is fully opened) in order to avoid having too much overall gain, although in the end the performance is not that much worse if all undulators are used. In the last stage for the 2 nm example, one can observe bunching generated at the edges of the region that experienced the first energy modulation. This may partly be a numerical artifact, but in any case it does not lead to significant radiation because the bunching is over a small region and incoherent. At 1 nm about 78% of the pulse energy is in the full largest spectral spike, while at 2 nm the corresponding number is 65%.

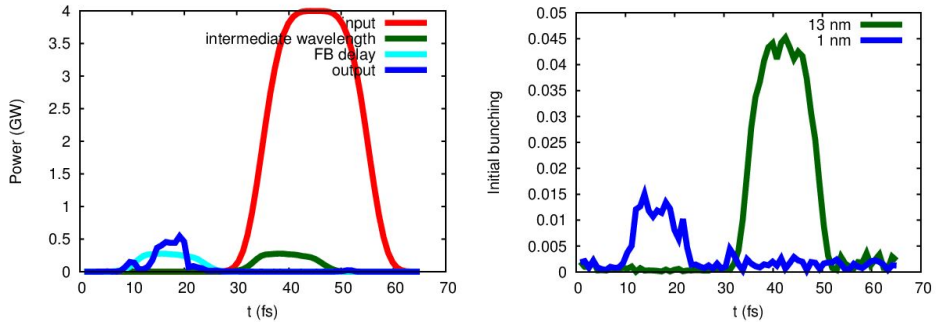

Figure 24: Cascaded HGHG to 1 nm. Temporal profile of the radiation at various stages and wavelengths (left), and initial bunching at the intermediate and final wavelengths (right).

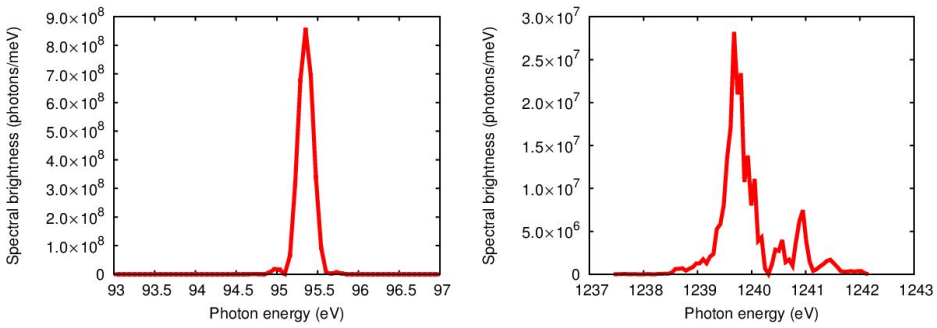

Figure 25: Cascaded HGHG to 1 nm. Spectrum of the radiation pulses at the intermediate wavelength (left) and the final wavelength (right). Note the significant degradation of spectral quality at the higher harmonic.

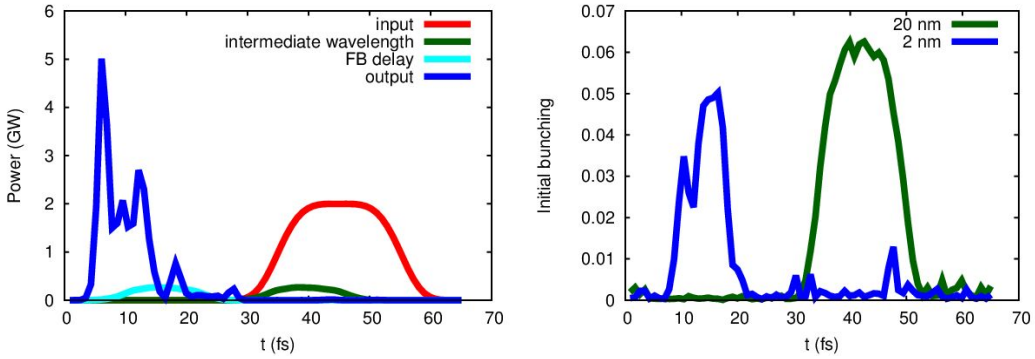

Figure 26: Cascaded HGHG to 2 nm. Temporal profile of the radiation at various stages and wavelengths (left), and initial bunching at the intermediate and final wavelengths (right).

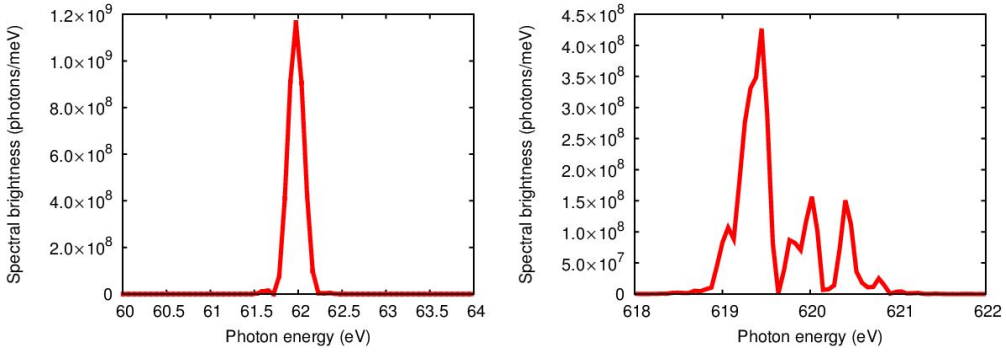

Figure 27: Cascaded HGHG to 2 nm. Spectrum of the radiation pulses at the intermediate wavelength (left) and the final wavelength (right).

EEHG

For the ideal short electron beam with a flat energy profile, the main impact of the large dispersion in EEHG is to stretch the beam by an amount that is proportional to the first energy modulation. This has the effect of transforming the initially flat current profile into a nearly triangular distribution with a strongly narrowed central lasing core. This shrinks the effective output pulse length, and broadens the spectrum compared to SXRSS. It also reduces the number of electrons that participate fully in the FEL amplification, (*i.e.*, the current is linearly reduced in the head and tail) so the total output power is reduced. The distortion is even stronger when generating bunching at shorter wavelengths. At 1 nm, the initial bunching is about 2%, while at 2 nm about 4% bunching is generated.

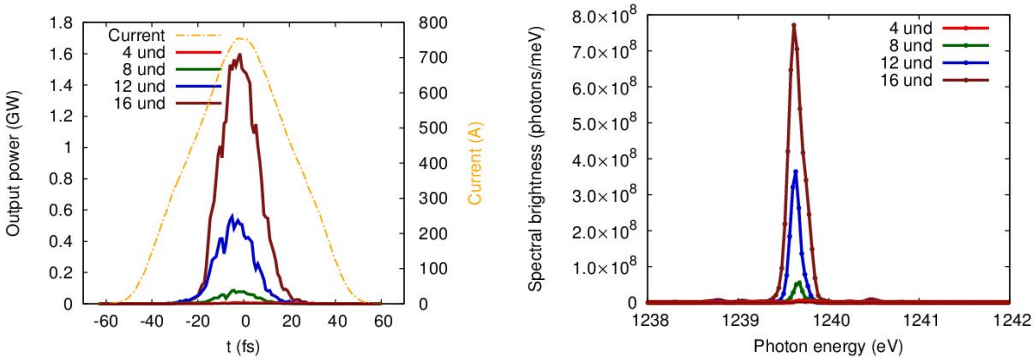

Figure 28: Power profiles overlaid with the final current profile (left) and spectra (right) at different positions along the radiating undulators for EEHG at 1 nm.

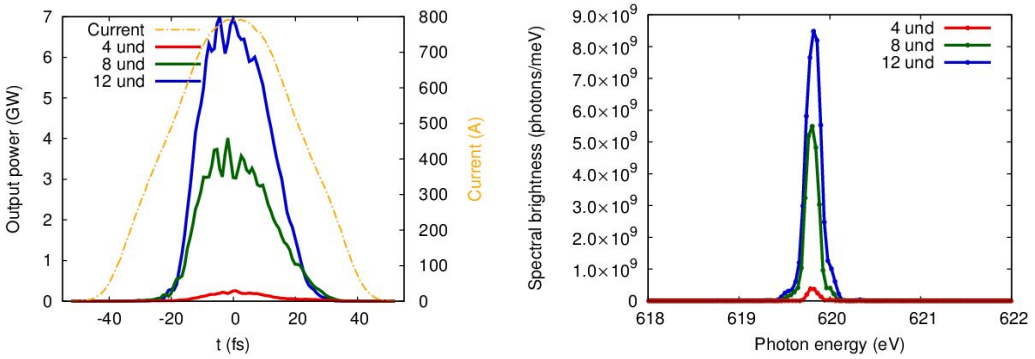

Figure 29: Power profiles overlaid with the final current profile (left) and spectra (right) at different positions along the radiating undulators for EEHG at 1 nm.

Simulations indicate that the ideal beams nevertheless produce single spike output spectra that are within three times the transform limit. The bandwidth broadening is due again primarily to the nonlinear wake in the undulator chamber, but because the induced chirp on the FEL pulse is nearly linear it may be partly removed by downstream optics.

In general, moderate initial energy modulations will not affect the EEHG scheme very much so long as they do not generate significant current spikes or folding over of the beam phase space. Examples where

a modest artificial energy modulation has been applied to the idealized electron bunch are given below for radiation at 1 nm after 16 undulator sections. The main impact is to slightly distort the profiles of the beam current, radiation power and spectrum, and to reduce the final pulse energy by 40% on average.

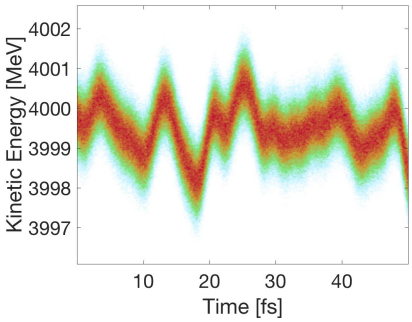

Figure 30: Example microbunching profile applied to the initial, ideal bunch.

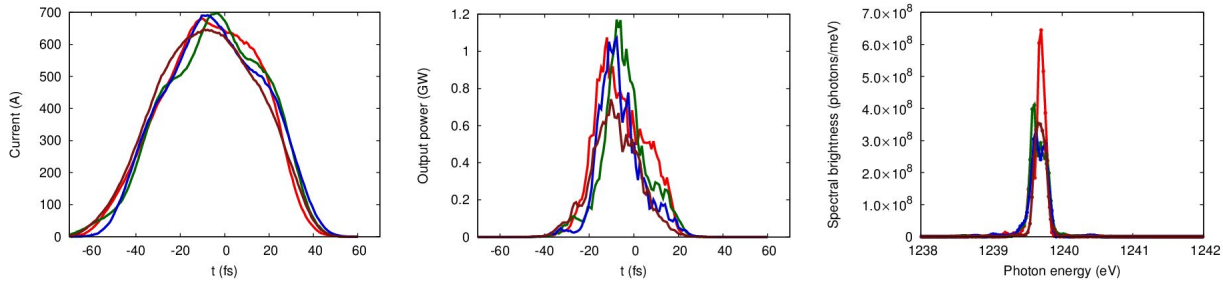

Figure 31: Profiles of the final current (left), power (center) and spectrum (right) for EEHG at 1 nm, with a different instance of artificial microbunching added for each curve shown.

Other Options for High-Brightness Operations

Several compelling alternatives to the primary seeding techniques are emerging as avenues to produce stable, narrowband pulses near the transform limit.

- *Hybrid EEHG/Cascaded EEHG/Echo-Fresh:* A straightforward extension to single stage EEHG is cascading multiple stages to reach 1 nm wavelength or shorter. Similar in concept to cascaded HGHG, but likely more stable, such schemes introduce added complexity to access EEHG control at short wavelengths.

- *RAFEL:* An interesting option in terms of potential FEL performance, the Regenerative Amplifier FEL (RAFEL) operates much like an FEL oscillator with cavity mirrors that recirculate a portion of the FEL output to re-seed trailing e-beam pulses. RAFELs operate in the high-gain regime (especially compared to normal oscillator configurations) and therefore need a relatively small number of passes (<few hundred) to reach steady state output levels. This significantly relaxes the alignment tolerances on the circulating seed. Preliminary studies on the RAFEL concept with the 1-MHz LCLS-II beam indicate intriguing near transform-limited operating modes in both soft and hard x-rays. However, the recirculation concept requires quite efficient optical transport in the

soft x-ray wavelength regime where in general grazing optics must be used.

- *Slippage-boosted spectral purification schemes:* A number of schemes like iSASE, pSASE, and harmonic lasing self-seeding can be used to clean the output FEL spectrum without the use of external seeding or monochromators. These schemes use enhanced slippage between the e-beam and the FEL light to moderately extend the effective coherence length of the pulse (typically gaining a factor of 2-3). While intriguing, this improvement alone does not reach the desired >10,000 resolving powers, but could be used in tandem with seeding. Nevertheless, most of these schemes required large tuning ranges in the undulator strengths or many chicane sections within the FEL for flexibility in wavelength. As such, there is limited applicability for implementation at LCLS-II in the present design.

Short Pulse (<15 fs) Operations

EEHG can be used to generate short x-ray pulses, down to 15 fs or even less for wavelengths longer than 1 nm. If the electron bunch itself is short, then there is a constraint that the combination of modulation and chicane will stretch the electron bunch, reducing the peak current and potentially increasing the duration of the x-ray pulse. To seed a short portion of a longer electron bunch, it is optimal to keep the first laser long enough to avoid generating a dip in the peak current following the first chicane while using the second laser to select a temporally narrow portion of the bunch. The pulse shortening effect is also strongest for the second seed laser. This configuration can lead to very short pulses, less than 10 fs for 2 nm, but tending to exacerbate the challenges in suppressing SASE from the unseeded portions of the bunch to produce sufficient contrast. It may be necessary to stop the amplification process before saturation is reached. In principle, only the external EEHG lasers need to be reconfigured to produce short pulses; however, it may be helpful to put effort into suppressing current spikes, or blowing up the energy spread in the head and tail of the bunch with, for example, temporally-shaped pulses in the laser heater.

Overlap With Other LCLS-II Programs & Infrastructure

High Average Power Laser Amplifier R&D

A major component of the required external seeding system is a high power laser capable of delivering up to 100 microjoule UV pulses, ideally at the full 1MHz electron beam repetition rate. The UV beam will likely be generated by tripling or quadrupling the output frequency of a suitable NIR/IR laser. Such a system is already under active development at SLAC as part of the High Average Power Laser Amplifier FEL R&D project. Several different laser configurations that closely align with the anticipated requirements of the seeding IR laser have been or will be built through this project, each aimed at addressing different needs of LCLS-II experiments and instruments, including the drive laser. Perhaps the simplest version of the FEL seeding laser system forms the pre-amplifier and high power amplifier pump system of the project's future OPCPA System (Optical Parametric Chirped-Pulse Amplification): a Tangerine fiber amplifier (Amplitude Systems, pre-amplifier pump) and Innoslab amplifier (Amphos, high power amplifier pump) that together produce 1.5-15 mJ, 1.5 ps pulses at 1.03 micron wavelengths at 0.1-1 MHz (1.5-2 kW average power). This system is the precursor to the LCLS-II photocathode drive laser system for which the pulses will be quadrupled to reach the same wavelengths required for FEL seeding. As such, there is a shared interest in the current effort to determine the performance of the frequency quadrupling system at high average power levels.

The 1.5 ps pulses are suitable, even ideal, for narrow band FEL seeding. The short pulse output of the OPCPA (ie, 15-200 fs) is also of interest for control of the FEL pulse length. One may envision either a

single or pair of seed laser systems that would enable great tunability in the coherent pulse length.

Spectral Phase Measurement and Control at High Rep Rate

A crucial element for the production of near transform-limited FEL pulses through external seeding is measurement and control of the seed laser spectral phase. There are numerous techniques for the generation of deep ultraviolet pulses, though many of the most efficient techniques are based on non-linear conversion of the typically near IR fundamental pulses to a low order harmonic (3-5). One key aspect is that the spectral phase of the seed laser pulses maps to phase-space modulation imprinted on the electron beam, but multiplied by the harmonic number. We foresee methods based on the generation of near transform limited early stage IR harmonics, *e.g.,* 2nd harmonic, and combining this with a spectrally shaped fundamental IR pulse to generate a combination frequency that is e.g. 2+2+1 for the 5th IR harmonic. By including one stage that is single photon mixed with a multi-photon preparation stage, we foresee the ability to linearly control the final spectral phase of the output pulse. A critical R&D step will thus be spectrogram measurement of the final deep-UV pulse. Initially designed as an integrating detections scheme, this would include a transient grating frequency resolved optical gating (tg-FROG) scheme for diagnostics, followed by a single-shot version made available for diagnosing the shot-to-shot stability of the controlled spectral phase. This high repetition rate diagnostic would then enable a wrapping of the spectral phase into a slow feedback loop that could correct for any anticipated dispersion drifts.

The proposed scheme for measuring a tg-FROG of the deep-UV pulses is nearly identical to the two dimensional method for measuring the arrival time of the x-ray pulses at LCLS. We can therefore leverage the effort for high repetition rate timing at LCLS-II, since both tasks require high repetition rate spectrogram diagnostics.

Optical Tailoring of e-beam

With the foresight of the LCLS-II repetition rate, we have recently demonstrated the ability to optically carve sections of the electron bunch by shaping dark solitons into the pulse temporal profile that is used as the photo-injector laser heater. The laser heater is nominally used to evenly heat the beam to suppress the development of MBI. However, we showed recently at LCLS that one can overdrive this heater in all but a narrow longitudinal slice of the bunch [A. Marinelli, et al, Phys. Rev. Lett. 116, 254801 (2016)]. This suppresses FEL lasing in all but the narrow slice region, which itself is only just heated to a level corresponding to optimal SXR lasing. Further, the shaped waveform can also be updated at high repetition rate, or wrapped into a feedback loop that modifies the details of the dark notch based on the high speed diagnostics downstream of the x-ray production.

XLEAP

The X-ray Laser-Enhanced Attosecond Pulse generation (xLEAP) project at LCLS is a laser-slicing system for the generation of sub-fs x-ray pulses up to 1 keV. The completed system will consist of a new magnetic chicane similar to the existing SXRSS chicane, a wiggler, a 2 μm laser, a laser safety system, and transport optics. The wiggler has a period of 33 cm and a tunable K parameter up to a value of 52. Installation of the beamline components in the LTU and lasers in B407 is currently underway, and testing using the LCLS electron beam will follow.

The xLEAP infrastructure will be used on the LCLS-II soft x-ray line. This program therefore has strong mutual overlap with potential future external soft x-ray seeding systems, including the location of the laser clean room, dedicated laser transport optics, diagnostics, undulator systems, and chicane. xLEAP

also enables opportunities to study the techniques of laser modulation and synchronization with the electrons, as well as the effect of the insertion devices on the beam. For example, the contribution to MBI by the strong xLEAP undulator and chicane can be studied near term to inform the design of seeding modulators and other lattice constraints. In terms of FEL performance at LCLS-II, an xLEAP system upstream of an EEHG seeding system suggests attractive new modes of seeded multicolor operations via three-wave mixing with both systems combined to produce controllable sidebands in the x-ray output. These are the subject of ongoing studies.

Upcoming Experimental Studies of External Seeding at Soft X-Rays

The current Task Force seeding effort builds on the historically strong SLAC involvement in seeded FEL research, including self-seeding at LCLS and the recent EEHG and HGHG proof of principle studies at NLCTA. Internationally, the FLASH (DESY), SXFEL (SINAP), and FERMI (Elettra) facilities are actively involved in laser seeding experiments, while groups in the UK and Switzerland are also actively involved in external seeding studies for the European XFEL and SwissFEL.

FLASH

The FLASH user facility at DESY houses sFLASH, an experimental setup for external seeding studies in the XUV to soft x-ray range. Typically sFLASH operates in single-stage HGHG mode with a 267 nm laser, but in principle the hardware also allows for EEHG studies. Recently, their group presented a set of reasonable parameters that would enable a first set of experimental EEHG tests in the XUV spectral regime [J. Boedewadt, et al, IPAC 2017]. The Task Force is actively collaborating with the sFLASH team on this effort.

FERMI

The FERMI FEL facility at Sincrotrone Trieste houses two FELs seeded by external UV lasers, and currently operates in High Gain Harmonic Generation (HGHG) mode to produce temporally coherent pulses with 10-100 fs duration. To produce longer wavelengths, FEL-1 covers the EUV 20-100 nanometer wavelength range, while FEL-2 uses two-stage HGHG to reach 4 nm.

FERMI recently began preparations to modify the FEL-2 beam line to enable dedicated EEHG studies in the 5-8 nm range beginning with a high power UV laser in the 260-nm wavelength region. These include installation of a new modulator, upgrade of the strong chicane, and second laser injection capabilities. Experiments are scheduled to begin in May 2018, with three periods (one week each) between May and June and two final periods (two weeks each) in July and August. At least one member of the Task Force will participate in each of these runs. The experiments will provide one-to-one comparisons between EEHG and cascaded HGHG. The goal is to determine the optimal seeding method based on several criteria such as stability, brightness, and reliability. Ideally, results will inform the future direction of the FELs at FERMI, as well as provide critical insight for seeding at LCLS-II.

We point out though that both this FERMI experiment and the one at SXFEL discussed in the next paragraph have certain limitations in comparison to EEHG operation at LCLS-II: 1) Both these experiments will be conducted at output wavelengths a factor of 5-10X longer than the desired 1 nm for LCLS-II, and there will be uncertainty in exactly how phase noise effects seen in the output spectra will

scale to the short wavelengths 2) Both experiments also use warm linac electron beams whose longitudinal phase spaces may be significantly worse in terms of stability, chirp, and microbunching noise than will (hopefully) be true for the LCLS-II beam. Consequently, either very good or disappointing results may not be directly extrapolable to LCLS-II in a quantitative sense. However, reasonable EEHG performance in either experiment would be a proof-of-principle result that would strongly suggest that given a sufficiently quiet electron and laser seed beam that EEHG can perform well in the 1-2 nm wavelength range.

SXFEL

The Shanghai X-ray FEL (SXFEL) at the Shanghai Institute of Applied Physics (SINAP) is a 840 MeV test facility currently under construction and designed to examine the principles of cascaded HGHG and EEHG [C. Feng et al., Science Bulletin 61, 1202 (2016)]. The baseline aims to produce 9 nm radiation from 265 nm lasers, either through two stage HGHG or through a EEHG-HGHG cascade. However, with the flexibility of the SXFEL layout, single stage EEHG at 9 nm can also be tested via different combinations of their several modulators and chicanes. It may also be possible to achieve EEHG at 3 nm via harmonic lasing.

Their current plan is to commission the beam line and do preliminary seeding experiments in late 2017, with the aim of reaching EEHG at 9 nm. Experiments will continue through early to mid 2018 in parallel with facility upgrades, and are intended to extend to studies of various cascading concepts to reach shorter wavelengths. The Task Force is collaborating in these efforts and will aim to participate in upcoming experiments as they bear on the seeding potential at LCLS-II.

Critical R&D

Given our current status and understanding of the available options for LCLS-II seeding, we identify several areas in need of further R&D. They include, but are not necessarily limited to:

- Experimental external seeding studies at FERMI and SXFEL, possibly elsewhere.
- Development of beam profile control and S2E beams that are better optimized for seeding. Methods to avoid the strong phase-space folding in EEHG will be explored, including under-compressed beams or the introduction of a negative R_{56} upstream.
- Detailed examination of the capability for enhanced control of FEL pulse, including tunable time-bandwidth trade-off, laser pulse shaping, and fast frequency tuning.
- Exploration of seeded multicolor operations, including coherent sideband production and control with beating of the laser heater and with the IR XLEAP laser, and/or with phase-locked multipulse operations with tunable temporal separation.
- Theoretical and simulational studies to quantify the contributions of impedances (e.g., resistive wall, CSR, LSC, MBI, etc) on electron beam and FEL output, and possible ways they can be mitigated.
- Continued exploration of feasibility of alternate seeding options at high rep-rate, such as the RAFEL.

Summary

High-resolution numerical simulations with recent S2E 100 & 300 pC beams for LCLS-II indicate that EEHG and SXRSS are both promising but challenging options to produce high brightness soft x-rays in

the 1-2 nm regime. SXRSS delivers pulses with B_e~2-20 times higher spectral brightness than EEHG, depending on the beam and on the tune. This is due to the increased energy spread of the laser modulated EEHG beam and the strong phase space deformation of the non-linear S2E beams in EEHG. EEHG, however, tends to produce cleaner spectra with narrower pedestals, and has greater potential flexibility for customized pulse tailoring. SXRSS has the obvious advantage of simplicity of setup (assuming cooling is adequate), but lacks some of the potential for multipulse and multicolor FEL operations enabled by external laser seeding. Thus, these seeding options appear to be complementary, given available space in the current LCLS-II beam line design, as well as expectations of user demand and FEL performance. The performance of these schemes with S2E beams that are better optimized for seeding is currently under study. We are also actively exploring alternate seeding options (*e.g.*, RAFEL) while preparing for external facility experimental tests of EEHG in the sub 10 nm regime through 2018.